Repetitive stimulation of autophagy-lysosome machinery by intermittent fasting preconditions the myocardium to ischemia-reperfusion injury

Rebecca J Godar,[1,2,†] Xiucui Ma,[1,2,†] Haiyan Liu,[1] John T Murphy,[1] Carla J Weinheimer,[1] Attila Kovacs,[1] Seth D Crosby,[3] Paul Saftig,[4] and Abhinav Diwan[1,2,*]

[1]Division of Cardiology and Center for Cardiovascular Research; Department of Internal Medicine; Washington University School of Medicine; St. Louis, MO USA; [2]John Cochran VA Medical Center; St. Louis, MO USA; [3]Department of Genetics; Washington University School of Medicine; St. Louis, MO USA; [4]Institut für Biochemie; Christian-Albrechts-Universität zu Kiel; Kiel, Germany

[†]These authors contributed equally to this work.

Keywords: autophagy, fasting, ischemia-reperfusion, lysosome, myocardial infarction

Abbreviations: CMA, chaperone-mediated autophagy; CQ, chloroquine; GFP, green fluorescent protein; LAD, left anterior descending; LAMP2, lysosomal-associated membrane protein 2; MOI, multiplicity of infection; NRCMs, neonatal rat ventricular cardiac myocytes; q4D, quaque qutra die/every fourth day; qOD, quaque otra die/every other day; TFEB, transcription factor EB; MAP1LC3B (also abbreviated as LC3), microtubule-associated protein 1 light chain 3, isoform B; TTC, triphenyl tetrazolium chloride; LV, left ventricle; AAR, area at risk; WT, wild type.

Autophagy, a lysosomal degradative pathway, is potently stimulated in the myocardium by fasting and is essential for maintaining cardiac function during prolonged starvation. We tested the hypothesis that intermittent fasting protects against myocardial ischemia-reperfusion injury via transcriptional stimulation of the autophagy-lysosome machinery. Adult C57BL/6 mice subjected to 24-h periods of fasting, every other day, for 6 wk were protected from in-vivo ischemia-reperfusion injury on a fed day, with marked reduction in infarct size in both sexes as compared with nonfasted controls. This protection was lost in mice heterozygous null for *Lamp2* (coding for lysosomal-associated membrane protein 2), which demonstrate impaired autophagy in response to fasting with accumulation of autophagosomes and SQSTM1, an autophagy substrate, in the heart. In *lamp2* null mice, intermittent fasting provoked progressive left ventricular dilation, systolic dysfunction and hypertrophy; worsening cardiomyocyte autophagosome accumulation and lack of protection to ischemia-reperfusion injury, suggesting that intact autophagy-lysosome machinery is essential for myocardial homeostasis during intermittent fasting and consequent ischemic cardioprotection. Fasting and refeeding cycles resulted in transcriptional induction followed by downregulation of autophagy-lysosome genes in the myocardium. This was coupled with fasting-induced nuclear translocation of TFEB (transcription factor EB), a master regulator of autophagy-lysosome machinery; followed by rapid decline in nuclear TFEB levels with refeeding. Endogenous TFEB was essential for attenuation of hypoxia-reoxygenation-induced cell death by repetitive starvation, in neonatal rat cardiomyocytes, in-vitro. Taken together, these data suggest that TFEB-mediated transcriptional priming of the autophagy-lysosome machinery mediates the beneficial effects of fasting-induced autophagy in myocardial ischemia-reperfusion injury.

Introduction

Therapeutic interventions to promote myocardial salvage in ischemia-reperfusion injury remain impractical, as they need to be applied before or simultaneously with onset of injury to achieve clinically significant reduction in cell death. Therefore, ongoing research efforts are focused upon preconditioning the myocardium to prevent cardiomyocyte death and/or dysfunction with myocardial infarction.[1] Contemporary approaches to ischemic preconditioning have limited translational application given

the unpredictability of spontaneous atherosclerotic plaque rupture and myocardial infarction. It is with this perspective that calorie restriction needs to be explored as a combinatorial strategy for prevention of cardiovascular events and preconditioning the myocardium to attenuate ischemia-reperfusion injury, if and when it were to occur.

Sustained calorie restriction attenuates atherosclerosis in humans;[2] markedly reduces the incidence of cardiovascular disease, diabetes and cancer; slows aging in primates;[3,4] and prolongs life span in multiple species.[5] Autophagy, an intracellular

lysosomal degradative pathway, plays a central mechanistic role in the life-span prolongation benefits of calorie restriction;[6] and pharmacologic induction of autophagy with rapamycin, resveratrol, and spermidine has similar effects in model organisms as *Drosophila melanogaster* and *Caenorhabditis elegans*.[7-10] Pertinent to this discussion is the observation that starvation (i.e. total calorie restriction) is a potent stimulus for induction of myocardial macroautophagy (henceforth referred to as 'autophagy').[11-13] Indeed, autophagy is essential for cardiac homeostasis in the perinatal starvation period at birth, prior to establishment of maternal milk supply; as mice with genetic ablation of autophagy proteins ATG5 and ATG7 cannot form autophagosomes and develop fatal myocardial ischemia.[14,15] Autophagy is also essential for maintenance of cardiac structure and function during prolonged starvation in mice, as concomitant impairment of autophagy with genetic ablation of *Foxo1*, haploinsufficiency of *Becn1*[11] or pharmacological inhibition with bafilomycin A_1,[16] an inhibitor of lysosome acidification and function, results in rapid development of cardiomyopathy with starvation. Activation of autophagy is also essential for cytoprotection during myocardial ischemia,[17] and pharmacologic stimulation of autophagy with rapamycin protects against postinfarction remodeling.[18] Myocardial autophagy is also induced with regimens of ischemic preconditioning;[19,20] and appears essential for the observed ischemic cytoprotection in ex-vivo ischemia-reperfusion injury.[19] Whether calorie restriction-induced autophagy confers ischemic cardioprotection is not known.

To overcome the behavioral challenges of maintaining persistent calorie restriction, periodic calorie restriction has been explored as a strategy to treat obesity;[21] and experimental studies have demonstrated life-span prolongation with intermittent fasting to an extent comparable to sustained calorie restriction in rodents.[22] Interestingly, intermittent fasting on an alternate day schedule preconditions the myocardium to cardiac ischemic injury with total coronary occlusion; and attenuates postinfarction remodeling.[23] In this study, we evaluated whether intermittent fasting stimulates cardiomyocyte autophagy-lysosome machinery as an essential mechanism for the observed cytoprotection against ischemia; and whether similar benefits are observed with reperfusion injury that often coexists with ischemic insult as a result of revascularization and is paradoxically suspected to be worsened by induction of autophagy.[17] Our data demonstrate a cyclical induction of autophagy with fasting accompanied by transcriptional induction of autophagy-lysosome machinery; and implicate a critical functional role for the autophagy-lysosome machinery in transducing the beneficial effects of intermittent fasting on ischemia-reperfusion injury.

Results

Intermittent fasting confers cardioprotection to ischemia-reperfusion injury

Previous studies have demonstrated a reduction in infarct size with attenuated post myocardial infarction remodeling and improved survival in rats subjected to every other day intermittent fasting for 3 mo, as compared to ad libitum fed rats followed by chronic total left anterior descending (LAD) coronary artery occlusion to create permanent ischemia.[23,24] To investigate whether reduced frequency of fasting or shorter duration of intermittent fasting regimens confer similar cardioprotection; and to determine whether the observed benefits extend to ischemia-reperfusion injury, we subjected adult male wild-type mice to 24 h of fasting on an every other day schedule (qOD; quaque otra die) for 2 and 6 wk; or on an every 4th d schedule (q4D; quaque qutra die) for 6 wk; and provided ad libitum access to standard chow to nonfasted controls; followed by ischemia-reperfusion modeling with reversible LAD ligation performed on a fed day to induce ischemia (30 min) followed by reperfusion (for 23.5 h; see **Fig. S1A** for experimental scheme). Intermittent fasting did not affect body weight (**Fig. 1A**), as mice commensurately increased their food intake on fed days (**Fig. 1B**), such that average food intake over a fasting-refeeding cycle was not different between any of the groups (**Fig. 1C**), as previously described.[25] Mice subjected to 6 wk of qOD intermittent fasting demonstrated a ~50% reduction in infarct size after ischemia-reperfusion injury, as compared with ad libitum fed controls (**Fig. 1D and E**); whereas shorter duration qOD regimen (for 2 wk) or a less frequent fasting schedule for the 6 wk duration did not confer similar cardioprotection. We confirmed that the observed reduction in infarct size with 6 wk of intermittent fasting was not related to differences in area at risk, with concomitant Evans Blue staining of nonischemic myocardium, in a separate cohort of mice (**Fig. 1F and G**).

Fasting-refeeding cycles modulate myocardial autophagy

Since fasting stimulates myocardial autophagy,[11-13,16] we evaluated cardiomyocyte autophagosome abundance in male mice carrying cardiomyocyte autophagy reporter GFP-tagged MAP1LC3B (green fluorescent protein-tagged microtubule-associated protein 1 light chain 3) transgene[13] subjected to intermittent (qOD) fasting for 6 wk (on a fed day). Mice subjected to 24 and 48 h of fasting, or to 24 h of fasting followed by 24 h of refeeding to mimic a fasting-refeeding cycle; and nonfasted age-matched controls were studied in parallel. Autophagosome abundance was not increased after a 24-h fast; but markedly increased after 48 h of fasting (**Fig. 1H and I**), which is consistent with previous observations[12,13,17] and suggests that 24 h of fasting induces autophagy with efficient flux (with prompt processing of autophagosomes). Indeed, assessment of autophagic flux by concomitant treatment with CQ (chloroquine) to inhibit lysosome acidification and prevent autophagosome processing;[26] and evaluate the ratio of autophagosomes (assessed with punctate GFP-LC3 imaging, **Fig. 1J**; and autophagosome-bound LC3-II by immunoblotting, **Fig. 1K and L**) and abundance of an autophagy substrate SQSTM1/p62 (**Fig. 1K and M**) in CQ-treated over diluent-treated animals, revealed marked enhancement of autophagic flux with 24 h of fasting as compared with basal state in nonfasted mice. Accumulation of autophagosomes after 48 h (**Fig. 1H and I**) likely reflects an imbalance between the rates of autophagosome generation and processing by the lysosomal machinery. Importantly, autophagosome accumulation was not

observed after a fed day in the mice subjected to 6 wk of every other fasting, mimicking the observations in mice refed for 24 h after a 24 h fast (**Fig. 1H and I**); and autophagic flux assessed with concomitant CQ treatment was not increased above the basal state observed in fed mice (**Fig. 1J–M**). These data indicate that intermittent fasting stimulates cardiomyocyte autophagy in a cyclical fashion with each episode of fasting, with return in autophagic flux to the basal levels on the fed days.

Intermittent fasting-induced protection against ischemia-reperfusion injury is lost in *Lamp2* heterozygous null mice, with impaired fasting-induced autophagy

To determine whether the lysosomal degradative machinery is essential for the observed benefits of intermittent fasting, we first studied mice with heterozygous ablation of *Lamp2*, an X-linked gene which encodes LAMP2 (lysosomal-associated membrane protein 2); loss of which results in impaired autophagosome-lysosome
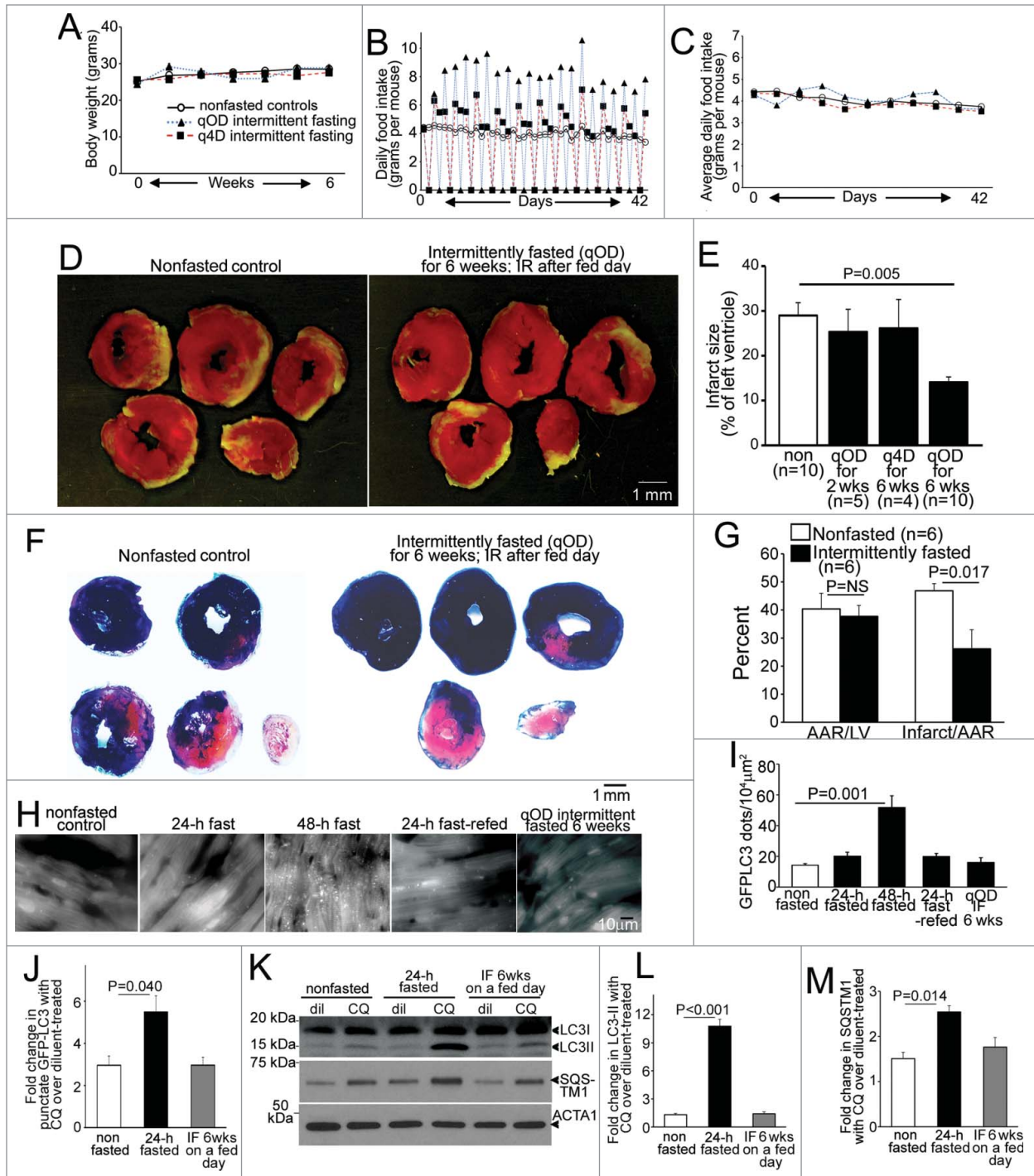

Figure 1. For figure legend, see page 1540.

Table 1. Morphometric and echocardiographic characteristics of *Lamp2* heterozygous null female mice at 8–10 wk of age, prior to starting intermittent fasting

	Littermate wild-type females	*Lamp2* het null females
Body weight (g)	17.0 ± 1.5	17.1 ± 0.5
Heart weight/body weight (mg/g)	5.3 ± 0.2	5.3 ± 0.2
LV end-diastolic diameter (mm)	3.13 ± 0.04	3.20 ± 0.04
LV end-systolic diameter (mm)	1.51 ± 0.01	1.46 ± 0.04
% LV fractional shortening	51 ± 1	54 ± 1
LV mass (mg)	78.1 ± 1.5	78.5 ± 2.3
Ratio of radius to wall thickness	1.97 ± 0.04	2.05 ± 0.05
Heart rate (beats per minute)	589 ± 29	616 ± 13

Data are reported as Mean $\pm$ SEM. N = 4–6/group for morphometric analysis and n = 3–4/group for echocardiographic characterization. No statistically significant differences were noted between the 2 groups by t-test.

fusion and Danon disease.[27] We examined the effects of partial loss of LAMP2 on autophagy in the myocardium, which is a critical lysosomal pathway stimulated in response to starvation,[11,14,15] and is impaired in mice with complete loss of LAMP2.[28] Female *Lamp2* heterozygous null mice (bearing the X/*null* genotype at the *Lamp2* locus), demonstrate no difference in body weight or heart weight (**Table 1**) as compared with littermate wild-type females. Interestingly, as compared with littermate wild-type mice, we observed a modest (but statistically nonsignificant) increase in punctate GFP-LC3 (**Fig. 2A and B**) and a significant increase in autophagosome-bound LC3-II (fold change: $2.4\pm$ vs.$1.0\pm$ in wild-type, $P < 0.001$, N = 5 /group; see **Fig. 2C**) and SQSTM1 (fold change: 1.3 ± 0.1 vs. 1.0 ± 0.1 in wild type, $P = 0.038$, N = 5 /group, see **Fig. 2C**), accompanied by a 53% reduction in myocardial LAMP2 protein (fold change: 0.47 ± 0.09 vs. 1.0 ± 0.03 in wild-type mice, $P = 0.008$, N = 5 /group; **Fig. 2C**), in the myocardium from 8-wk-old *Lamp2* heterozygous null mice. To determine if this was as a result of impaired autophagic flux with *Lamp2* deficiency, we treated a cohort of 8-wk-old *Lamp2* heterozygous null and littermate wild-type mice with CQ (or diluent) in the fed state and assessed the ratio of autophagosome-bound LC3-II and SQSTM1 in CQ-treated over diluent-treated mice as an index of autophagic flux. As observed in the male mice (**Fig. 1K, L and M**), CQ treatment resulted in accumulation of LC3-II and

SQSTM1 in wild-type female myocardium indicating intact basal autophagic flux (**Fig. 2D**). Interestingly, autophagic flux was not significantly different in hearts from nonfasted *Lamp2* heterozygous null mouse hearts as compared with nonfasted wild-type littermates, suggesting that the reduced levels of LAMP2 in *Lamp2* heterozygous null mice were sufficient to maintain basal autophagic flux in the myocardium (**Fig. 2D and E**). It is conceivable that the observed accumulation of autophagosomes in the fed state in *Lamp2* heterozygous null females is due to mosaic loss of *Lamp2* allele due to random X chromosome inactivation in cells and tissues.[27,29] Importantly, the observed autophagosome accumulation in *Lamp2* heterozygous null mouse myocardium did not impair resting cardiac structure and function in these mice in the unstressed state as compared with littermate wild types (**Table 1**) confirming previous observations.[28,30]

We next examined whether heterozygous ablation of *Lamp2* affects autophagic flux under fasting stress. Indeed, as compared with littermate wild-type females, the accumulation of GFP-LC3-labeled autophagosomes was markedly worsened when *Lamp2* heterozygous null females were subjected to 48 h of fasting (**Fig. 2A and B**); with progressive accumulation of autophagosome-bound LC3-II, SQSTM1 (a receptor protein which is also a substrate for autophagy;[31] **Fig. 2C**) and polyubiquitinated proteins (which accumulate with autophagy impairment;[32]

Figure 1 (See previous page). Intermittent fasting confers protection to ischemia-reperfusion injury in wild-type mice, with upregulation of autophagic flux on fasting days. (**A–C**) Mean body weight (**A**), average daily food intake (**B**) and daily food intake averaged over each fasting-refeeding cycle (**C**) in adult male C57BL/6 mice subjected to every other day fasting (qOD, n = 21; *black triangles and blue dotted line*); every 4th day fasting (q4D, n = 5 ; *black squares and red dashed line*); and nonfasted (ad libitum fed) controls (n = 20 ; *open circles and bold black line*). (**D**) Representative images of TTC-stained sections of hearts (at 24 h after surgical modeling) from intermittently fasted (for 6 wk) and nonfasted male mice (as controls) subjected to reversible LAD ligation for 30 min followed by reperfusion on a fed day. (**E**) Infarct size (at 24 h), quantified as unstained area (white)/total left ventricular myocardial area in male mice subjected to LAD territory ischemia (30 min) followed by reperfusion on a fed day, after intermittent fasting on a q4D schedule (for 6 wk) or qOD schedule for 2 or 6 wk as compared to nonfasted (ad libitum) fed controls (as in A to C). P value depicted is by post-hoc test after one-way ANOVA. (**F and G**) Representative images of TTC and Evans blue-stained sections of hearts subjected to ischemia-reperfusion (IR) injury, as in (**D**), on a fed day after 6 wk of intermittent fasting (or ad libitum feeding as control; F), with quantification of area-at-risk (AAR) and infarct size as a percent of AAR (**G**). *P* value is by t test. (**H, I**) Representative gray-scale images (at 630X magnification; **H**) and quantification of punctate GFP-LC3 (autophagosomes; **I**) in mice with cardiomyocyte-specific expression of GFP-LC3 after various durations of fasting, refeeding and intermittent fasting (for 6 wk, assessed on a fed day). N = 3 or 4/group. (**J**) Assessment of autophagic flux by ratio of punctate GFP-tagged LC3 in mice subjected to 24 h of fasting, 6 weeks of intermittent fasting (IF) on a fed-day or provided ad libitum access to food (nonfasted) and treated with chloroquine (CQ) or diluent, 4 h prior to sacrifice (n = 3 or 4/group). (**K**) Representative immunoblot depicting endogenous LC3 and SQSTM1 in mice treated as in J. (**L and M**) Assessment of autophagic flux by ratio of LC3-II (**L**) or SQSTM1 (**M**) in CQ versus diluent-treated mice, modeled as in (**J**). N=3 /group. *P* values depicted are by post-hoc test after one-way ANOVA in I to M.
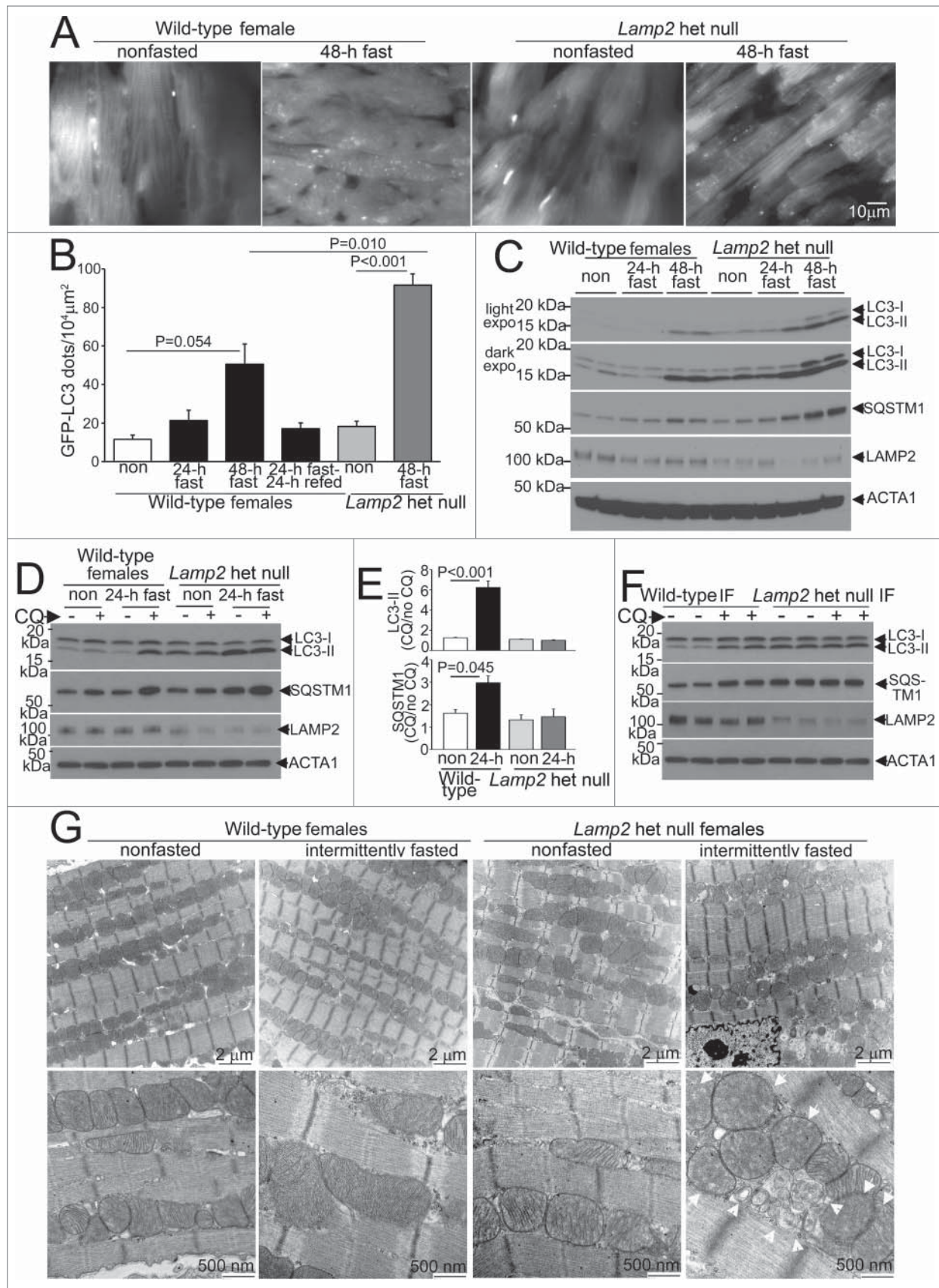
Figure 2. For figure legend, see page 1542.

Table 2. Morphometric and echocardiographic characteristics of *Lamp2* heterozygous null female mice subjected to 6 wk of intermittent fasting, on a fed day

	Littermate wild-type females	*Lamp2* het null females
Body weight (g)	18.4 ± 0.8	18.8 ± 0.6
Heart weight/body weight (mg/g)	5.1 ± 0.3	5.5 ± 0.2
LV end-diastolic diameter (mm)	3.09 ± 0.09	3.28 ± 0.03
LV end-systolic diameter (mm)	1.48 ± 0.04	1.82 ± 0.04*
% LV fractional shortening	52 ± 1	45 ± 1*
LV mass (mg)	72.6 ± 3.22	79.2 ± 0.7
Ratio of radius to wall thickness	2.03 ± 0.13	2.15 ± 0.03
Heart rate (beats per minute)	599 ± 14	599 ± 44

Data are reported as Mean ± SEM. N = 4/group.
*Indicates $P < 0.05$ by t-test. LV, left ventricle.

Fig. S2) in the *Lamp2* heterozygous null myocardium, provoked by increasing duration of fasting. Indeed, while 24 h of fasting significantly upregulated autophagic flux in wild-type female mice as compared to the nonfasted controls (mimicking the observations in male mice, **Fig. 1K–M**), fasting did not further stimulate autophagic flux above the basal state in the *Lamp2* heterozygous null mice (**Fig. 2D and E**). These data suggest that the consequences of LAMP2 deficiency (in *Lamp2* heterozygous null mice) on global autophagic flux are only unmasked in the presence of a stressor such as fasting, which rapidly stimulates formation of autophagosomes, which are thereafter not processed efficiently, due to impaired autophagosome-lysosome fusion. Therefore, *Lamp2* heterozygous null mice are well suited as a model system to evaluate the effects of impaired myocardial lysosome function and consequently impaired autophagy specifically under stress; as they do not display the disadvantages observed in other model systems employed to study the effects of impaired autophagy-lysosomal machinery, namely presence of cardiomyopathy in the unstressed state (as in mice with cardiac myocyte specific or germline ablation of proteins essential for autophagosome formation, ATG5, ATG7, and PIK3C3;[14,15,33,34] and in models of lysosomal dysfunction [reviewed in ref. 35]); or the paradoxical effects on autophagy observed with haploinsufficiency of BECN1.[13,17,36]

To determine if LAMP2 deficiency impairs autophagic flux with repetitive fasting, we subjected *Lamp2* heterozygous null mice and littermate wild types for 6 wk of intermittent fasting followed by assessment of autophagic flux with injection of CQ (or diluent) on a fed day. *Lamp2* heterozygous null mice demonstrated impaired autophagic flux on a fed day after being subjected to the intermittent fasting protocol, assessed as CQ-induced accumulation of LC3-II (fold change in CQ/dil over nonfasted mice: 0.97 ± 0.06 vs.1.87 ± 0.32 in wild types, $P = 0.036$, N = 4 /group, **Fig. 2F**) and SQSTM1 (fold change in CQ/dil over nonfasted mice: 0.95 ± 0.16 vs.1.46 ± 0.01 in wild types, $P < 0.001$, N = 4 /group, **Fig. 2F**). This was associated with accumulation of autophagic structures (arrowheads, **Fig. 2G**) and abnormal appearing mitochondria with rarified cristae architechture (arrows) on transmission electron microscopy analysis in *Lamp2* heterozygous null mice (and not wild-type controls) subjected to intermittent fasting for 6 wk, on a fed day. At this time point, we also observed impaired left ventricular ejection performance on echocardiographic assessment in intermittently fasted *Lamp2* heterozygous null mice (with increased left ventricular end-systolic diameter and reduced % fractional shortening as compared with similarly treated wild type, see **Table 2**) which is not observed in ad libitum fed *Lamp2* heterozygous null females at this age (data not shown). Taken together, these data indicate that intermittent fasting-induced impairment of autophagic flux results in accumulation of abnormal mitochondria, which require intact autophagy-lysosomal machinery for their removal,[37] with consequent deterioration of myocardial function.

Importantly, intermittent fasting conferred cardioprotection in wild-type female mice, with a ~50% reduction in infarct size as compared with nonfasted matched controls (**Fig. 3A and B**),

Figure 2 (See previous page). Intermittent fasting is associated with impaired autophagic flux in *Lamp2* heterozygous null mice. (**A**) Representative gray-scale images (at 630X magnification) of female *Lamp2* heterozygous null and littermate wild-type female mice bearing the GFP-LC3 transgene, after 48 h of fasting or in a fed (nonfasted) state. (**B**) Quantification of cardiomyocyte GFP-LC3 in *Lamp2* heterozygous null mice or littermate control females after fasting and/or refeeding for the indicated duration; n = 3 or 4/group. *P* values depicted are by post-hoc test after one-way ANOVA. (**C**) Immunoblots depicting LC3 processing and SQSTM1 accumulation in *Lamp2* heterozygous null mice with progressively longer periods of fasting, as compared with nonfasted littermate wild-type female controls. ACTA1 was employed as loading control. (**D and E**) Representative immunoblots (**D**) and quantification of ratio of LC3-II (**E**, *top*) and SQSTM1 (E, *bottom*) in cardiac extracts from *Lamp2* heterozygous null mice and female littermate wild-type controls subjected to 24 h fasting or provide ad libitum access to diet and treated for CQ or diluent (for 4 h prior to sacrifice). N = 3 /group. *P* values are by post-hoc test after one-way ANOVA. (**F**) Representative immunoblots depicting LC3 and SQSTM1 in *Lamp2* heterozygous null mice and female littermate wild-type mice subjected to intermittent fasting for 6 wk, and treated for CQ or diluent (for 4 h prior to sacrifice) on a fed day. (**G**) Representative transmission electron microscopy images of cardiac tissues from *Lamp2* heterozygous null mice and female littermate wild-type mice subjected to intermittent fasting, or provided ad libitum access to food for 6 wk, on a fed day. N = 3 /group. Arrows indicate mitochondria with loss of cristal architecture, and arrowheads point to autophagic structures.

which was not due to differences in area at risk (**Fig. 3C and D**), paralleling the observations in male mice (**Fig. 1D–G**); and this cardioprotection was lost in *Lamp2* heterozygous null mice (**Fig. 3A–D**). Taken together, these data indicate that the impairment in autophagic flux with each fasting episode in *Lamp2* heterozygous null mice results in accumulation of damaged mitochondria, with impaired basal autophagic flux even on a fed day after 6 wk, likely resulting in the loss of cardioprotection observed with this regimen in wild-type mice.

Intermittent fasting induces adverse ventricular remodeling and cardiomyocyte death in *lamp2* null mice, associated with impaired autophagic flux

We next examined the effects of intermittent fasting on the myocardium with complete loss of LAMP2. *lamp2* null mice demonstrate increased mortality in the neonatal period with autophagosome accumulation in cardiomyocytes and multiple other tissues with multisystem abnormalities;[28] and surviving *lamp2* null mice demonstrate cardiomyopathy with impaired cardiac and myofiber contractility at ~6 mo of age,[30] mimicking the observations of cardiomyopathy in humans with Danon disease and hypertrophic cardiomyopathy resulting from mutations in the *LAMP2* gene and loss of the LAMP2 protein.[27] To determine if repetitive stimulation of autophagosome formation with fasting affects the development of cardiomyopathy in the absence of LAMP2, we subjected 8- to 10-wk-old (young adult) male *lamp2* null mice and littermates to intermittent fasting, with serial weekly echocardiographic determination of cardiac structure and function, before and during, and immediately after the period of intermittent fasting. At this age, surviving *lamp2* null

mice demonstrated cardiomyocyte autophagosome accumulation (**Fig. 4A and B; Fig. S3**), as previously described,[28] with accumulation of SQSTM1, an autophagy substrate in the myocardium (**Fig. 4A and B**). Importantly, assessment of autophagic flux with CQ (or diluent) treatment revealed that basal autophagic flux was impaired in *lamp2* null mice in the fed state (in contrast to intact flux in littermate wild types, **Fig. 4A and B**), prior to initiation of the intermittent fasting protocol. Intermittent fasting provoked further accumulation of autophagosome-bound LC3-II (**Fig. 4D and E**) and SQSTM1 (**Fig. 4D and F**) in intermittently fasted *lamp2* null mice on a fed day, as compared with ad libitum fed *lamp2* null mice as well as intermittently fasted wild-type controls (**Fig. 4D–F**), indicating impaired autophagy resulting from impaired autophagosome-lysosome fusion in the absence of LAMP2. Myocardial ultrastructure examination at this point in time revealed accumulation of autophagosomes in ad libitum fed *lamp2* null mice (as compared with wild-type controls in either group; arrowheads, **Fig. 4G**), which was markedly worsened with appearance of damaged mitochondria (appearing swollen with loss of cristal architecture, arrows) in intermittently fasted *lamp2* null mice.

Interestingly, surviving young adult *lamp2* null mice did not demonstrate significant echocardiographic changes in cardiac structure and function as compared with controls (**Fig. 5A–D**), before initiation of the intermittent fasting regimen. Importantly, while intermittent fasting did not affect cardiac structure or function or organ weights in wild-type mice, as compared with ad libitum fed wild-type mice (**Fig 5A–E; Table 3**), the repetitive fasting protocol provoked progressive left ventricular dilation (**Fig. 5A and B**), decline in ejection performance (**Fig. 5A and**
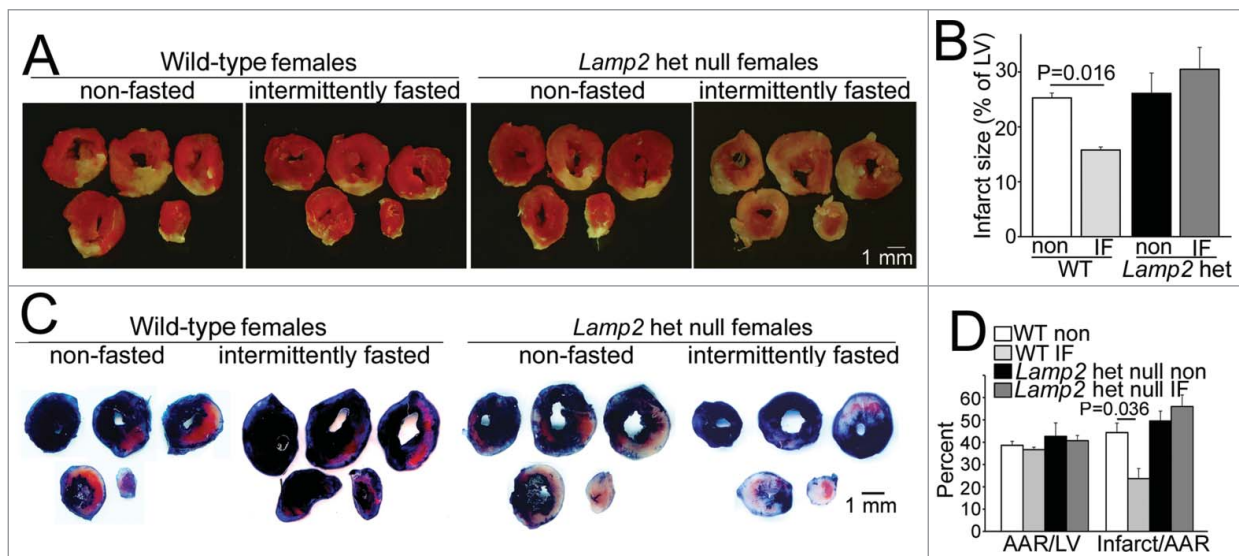

Figure 3. Intermittent fasting does not confer protection to cardiac ischemia-reperfusion injury in *Lamp2* heterozygous null mice. (**A and B**) Representative images of TTC-stained sections of hearts (**A**) and infarct size (at 24 h, **B**) after in vivo LAD territory ischemia (30 min) followed by reperfusion in *Lamp2* heterozygous null mice and littermate wild-type (WT) females subjected to intermittent fasting for 6 wk (with surgical modeling on a fed day) or provided ad libitum access to standard chow; n = 4 to 7/group. *P* values depicted are by post-hoc test after one-way ANOVA. (**C and D**) Representative images (**C**) of hearts stained with Evans blue to determine area at risk (AAR, quantified in **D**) simultaneously with TTC staining to assess infarct size (quantified as fraction of AAR, **D**) in mice modeled as in A. N = 3 to 6/group. *P* values depicted are by post-hoc test after one-way ANOVA. LV, left ventricle.

C) and progressive increase in left ventricular mass (**Fig. 5A and D**) with increased heart weight; and increased liver and lung weights (suggesting presence of heart failure with congestion,

Table 3) in *lamp2* null mice after 5 wk, with clinical signs of heart failure (such as hunched posture and labored breathing) observed in some animals. Importantly, these findings were not
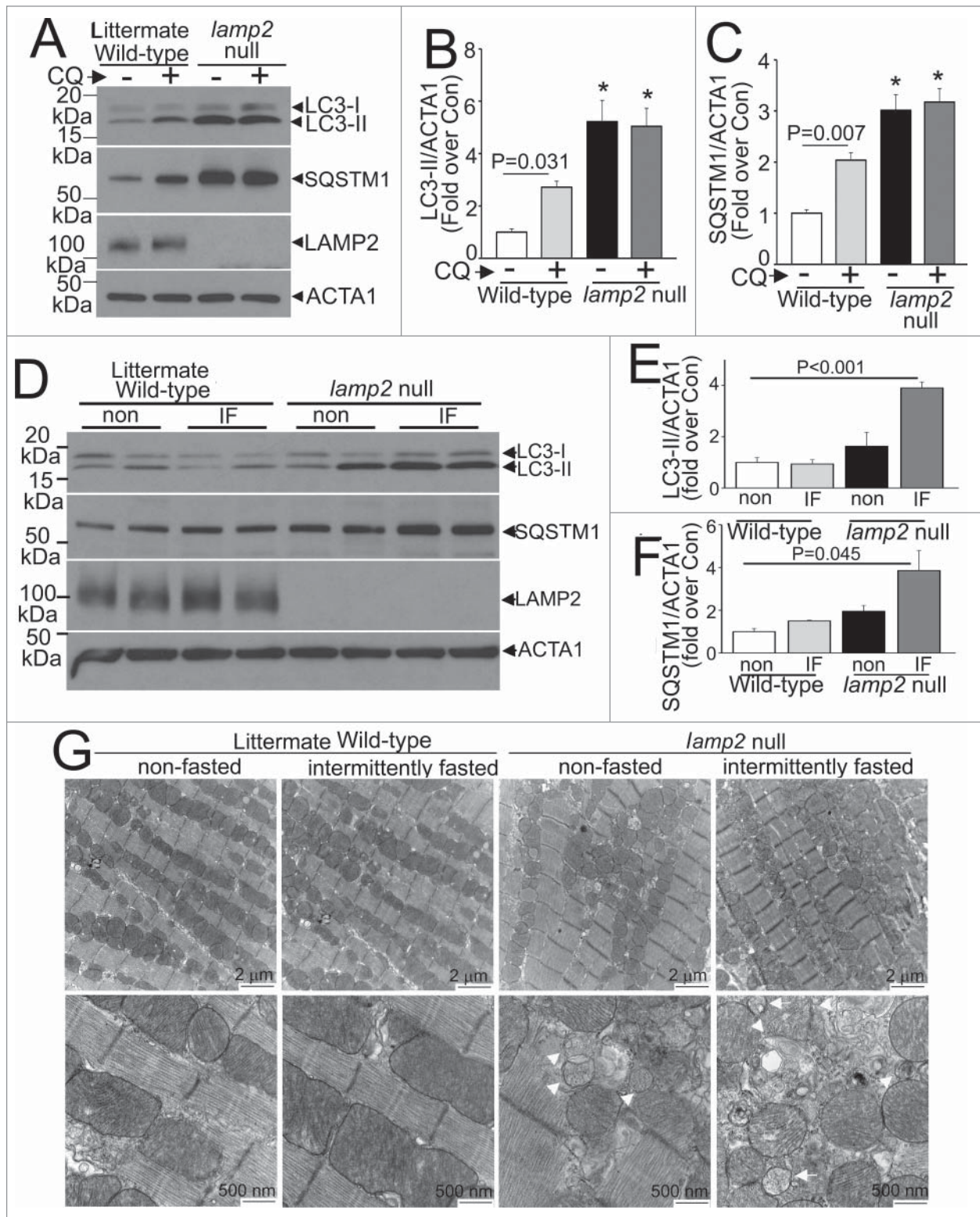

Figure 4. For figure legend, see page 1545.

accompanied by a change in body weight (**Fig. 5E**, **Table 3**), or spontaneous development of cardiomyopathic changes in ad libitum fed *lamp2* null mice followed for the same period (**Fig. S4**), as compared with similarly treated age-matched wild-type controls. We also observed increased cardiomyocyte cell death, with increased evidence for programmed apoptosis (TUNEL positivity, **Fig. 6A and B**) and necrosis (c5b-9 positivity, **Fig. 6C and D**) in intermittently fasted *lamp2* null mice, as compared with ad libitum fed *lamp2* null or wild-type mice from both ad libitum and intermittently fasted groups; as the likely mechanism for the observed adverse ventricular remodeling in these mice. Taken together, these data indicate an essential role for the lysosome machinery in maintaining autophagic flux, cardiomyocyte viability, and cardiac structure and function during intermittent fasting. Not surprisingly, therefore, intermittent fasting did not confer cardioprotection to ischemia-reperfusion injury in the *lamp2* null mice (**Fig. 6E and F**); which was confirmed with markedly increased left ventricular infarct size despite comparable area-at-risk in intermittently fasted *lamp2* null mice as compared with similarly treated littermate controls (**Fig. 6G and H**).

Intermittent fasting modulates oxidative stress in the myocardium

Our observations indicate that whereas autophagic flux was not upregulated on a fed day after a 6-wk period of intermittent fasting (above the basal levels), a remarkable (∼50%) infarct size reduction was observed in wild-type mice subjected to ischemia-reperfusion injury at this time (**Figs. 1D–G and 3**), indicating the intermittent fasting preconditions the myocardium to the upcoming injury. Since ablation of LAMP2 prevented this preconditioning effect with accumulation of abnormal mitochondria (**Figs. 2G, 3, 4G, and 6E–H**), and damaged mitochondria provoke increased generation of reactive oxygen species (ROS) in the myocardium,[38] we hypothesized that intermittent fasting regulates myocardial ROS generation via effects on mitochondria, which is lost in the setting of *Lamp2* ablation due to impairment in mitochondrial autophagy. Indeed, we observed a significant reduction in myocardial levels of oxidatively modified proteins in intermittently fasted wild-type mice of both sexes as compared with ad libitum fed controls (**Fig. 7A–D**), suggesting that intermittent fasting lowers myocardial ROS levels. Importantly, the abundance of oxidatively modified proteins was markedly increased in heterozygous *Lamp2* null as well as *lamp2* null myocardium (**Fig. 7A–D**), with further worsening upon intermittent fasting in the *Lamp2* heterozygous null mice (**Fig. 7A and C**), paralleling the observed impairment in autophagic flux with

accumulation of abnormal appearing mitochondria in these models. Taken together, these observations suggest that intermittent fasting preconditions the myocardium via enhanced autophagy of damaged mitochondria,[39] with consequent reduction in oxidative stress.

Chaperone-mediated autophagy (CMA) is another well described lysosomal degradative pathway that is postulated to be impaired in mice with deficiency of LAMP2A isoform.[40] This pathway has been shown to be activated in the myocardium by fasting, in vivo, and by oxidative stress.[41] To examine its role in intermittent-fasting induced cardioprotection, we assessed the abundance of candidate proteins that are known chaperone-mediated autophagy substrates[40] in the myocardium, in these models. Interestingly, our data do not demonstrate any significant alteration in abundance of these proteins with intermittent fasting or *Lamp2* ablation (which also results in loss of the LAMP2A isoform;[28] see **Fig. S5**), which suggests that alterations in CMA are unlikely to play a central role in transducing the cardioprotective benefits of intermittent fasting.

Given that autophagy plays an essential role for removal of damaged mitochondria during starvation,[42,43] we hypothesized that repetitive enhancement of autophagy would reduce prevalence of depolarized mitochondria; whereby simultaneous inhibition of autophagy would provoke accumulation of depolarized mitochondria. To test this hypothesis, we subjected neonatal rat ventricular cardiac myocytes (NRCMs) to 2 12-h periods of starvation, interspersed with 12 h periods of exposure to a nutrient-rich environment (see schematic in **Fig. S1B**), in the presence of shRNA targeting *Becn1* (to inhibit autophagosome formation), *Lamp2* (to inhibit autophagosome-lysosome fusion) and sh*LacZ* as control; and evaluated mitochondrial quality, mass, and ultrastructure. As shown, near-complete knockdown of BECN1 prevented LC3-II generation with accumulation of SQSTM1 (**Fig. 8A**), whereas knockdown of LAMP2 resulted in accumulation of autophagosome-bound LC3-II and SQSTM1 (**Fig. 8B**) confirming the inhibition of macroautophagy. Repetitive starvation resulted in significant reduction in prevalence of depolarized mitochondria assessed with JC-1 fluorescence (**Fig. 8C and D**), without a change in mitochondrial mass (**Fig. 8E**) and with preserved mitochondrial ultrastructure (**Fig. 8F**). In contrast, inhibition of autophagy with either BECN1 or LAMP2 knockdown resulted in increased prevalence of depolarized mitochondria; which was significantly worsened in cells subjected to repetitive starvation (**Fig. 8C and D**) consistent with lack of removal of starvation-damaged mitochondria when the autophagy-lysosome machinery was inhibited in this setting. Indeed, mitochondrial

Figure 4 (See previous page). Intermittent fasting (IF) worsens the autophagic impairment observed in *lamp2* null mice. (**A**) Representative immunoblot depicting LC3 processing and SQSTM1 in cardiac extracts from young adult *lamp2* null males (and littermate wild-type controls) treated with CQ or diluent to assess autophagic flux. (**B and C**) Quantification of LC3-II (**B**) and SQSTM1 (**C**) in mice treated as in A. N = 4 /group. * indicated $P < 0.05$ versus diluent treated wild-type control. *P* values are by one-way ANOVA. (**D–F**) Representative immunoblots (**D**) with quantitative analysis of LC3-II (**E**) and SQSTM1 (**F**) in *lamp2* null mice subjected to intermittent fasting (for 5 wk) as compared with similarly treated littermate controls, and age-matched nonfasted *lamp2* null and littermate wild-type mice. N = 4 to 6/group. *P* values depicted are by post-hoc test after one-way ANOVA. (**G**) Representative transmission electron microscopy images of cardiac tissues from *lamp2* null mice and littermate wild-type mice subjected to intermittent fasting, or provided ad libitum access to food for 5 wk, on a fed day. N = 3 /group. Arrows indicate mitochondria with loss of cristal architecture, and arrowheads point to autophagic structures.
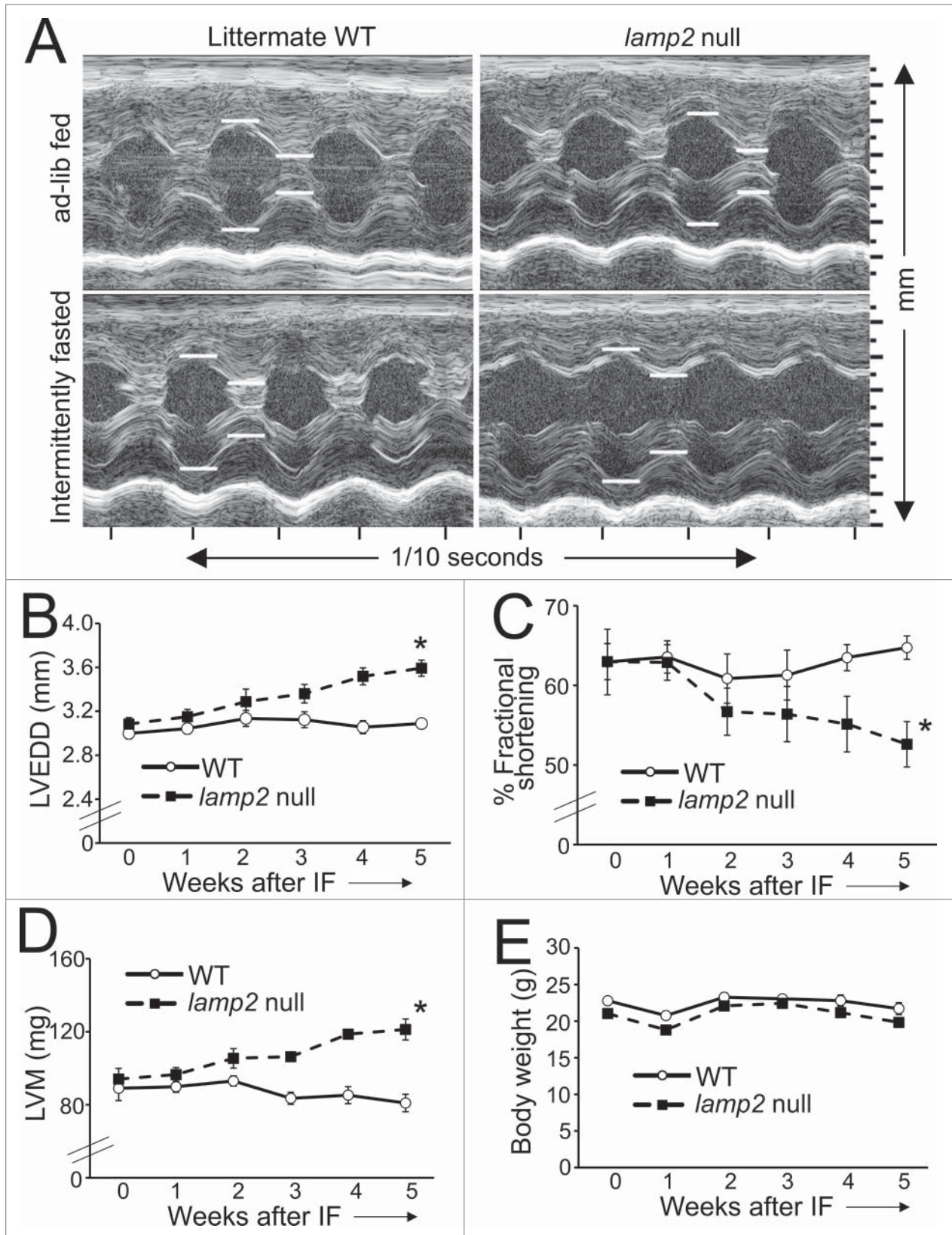
Figure 5. For figure legend, see page 1547.

Table 3. Morphometric data on *lamp2* null male mice subjected to intermittent fasting for 5 wk

	Body weight (g)	Heart weight (mg)	Liver weight (mg)	Lung weight (mg)
Wild type not fasted (n = 6)	22.7 ± 1.2	115.1 ± 5.2	1109 ± 39	175 ± 12
Lamp2 null not fasted (n = 6)	22.0 ± 0.8	128.8 ± 5.9	1108 ± 32	175 ± 9
Wild type intermittently fasted (n = 5)	21.7 ± 0.8	112.3 ± 8.3	885 ± 59	160 ± 5
Lamp2 null intermittently fasted (n = 7)	19.8 ± 0.3	136.4 ± 2.9[P = 0.035]	1166 ± 77[P = 0.014]	203 ± 8[P = 0.024]

All data are shown as Mean ± SEM. P values shown are for comparision with wild type intermittently fasted group by post-hoc test after one-way ANOVA.

mass was also increased with autophagy inhibition (**Fig. 8E**). Also, ultrastructural analysis demonstrated structurally damaged mitochondria, which appeared fragmented with BECN1 knockdown; and swollen with loss of cristal architecture and within autophagosomes with LAMP2 knockdown (**Fig. 8F**). These findings are consistent with a preconditioning effect of repetitive starvation on the cells with improved mitochondrial quality (as observed in vitro, **Fig. 8**) and reduced ROS (as observed in vivo, **Fig. 7**), in a manner dependent upon presence of an intact autophagy-lysosome machinery.

Fasting and refeeding transcriptionally modulate the autophagy-lysosome machinery

Consumption of lysosomes and components of the autophagy machinery occurs with starvation-induced autophagy; with prompt replenishment observed with continued starvation stress.[44] To determine the transcriptional regulation of autophagy-lysosome proteins in response to fasting, in vivo, we performed quantitative PCR analysis for candidate autophagy-lysosome genes. Our data demonstrate a robust transcriptional induction of *Map1lc3b, Sqstm1, Lamp2a*, and *Lamp2b* isoforms, with a strong trend toward upregulation of *Becn1* and *Lamp1* after 24 h of fasting (as compared with nonfasted controls; **Fig. 9A–F**). Although, we did not observe transcriptional regulation of *Gapdh* in the fasted myocardium; we also confirmed the observations with *Rpl32* coding for a ribosomal protein, employed as a housekeeping control; and found significant transcriptional induction of *Becn1* and *Lamp1* too, in myocardium from mice subjected to a 24-h fast as compared with nonfasted controls (**Fig. S6A and B**). Refeeding fasted mice (for 24 h) restored the expression of these candidate gene transcripts to levels comparable to or lower than those observed in nonfasted mice. Importantly, longer durations of fasting (48 h) or intermittent fasting for 3 or 6 wk did not upregulate the expression of these candidate genes on a fed day; as compared with matched ad libitum fed controls. These data attest to a tight transcriptional regulation of autophagy-lysosome machinery in the myocardium that closely tracks activation of autophagy with fasting and decline to basal levels (or below) with refeeding. We next

examined the abundance of proteins coded for by these transcripts. Fasting for 24 h increased the ratio of LC3-II to LC3-I implying induction of autophagy (**Fig. 10A and B**), without a change in the abundance of any of the proteins evaluated, as compared with the nonfasted state (**Fig. 10A–F**). Concomitant treatment with CQ revealed significantly increased abundance of total LC3 (1.91 ± 0.26 fold, N = 3 /group, P = 0.028, see **Fig. 1K**) and SQSTM1 (3.01 ± 0 .fold13-, N = 3 /group, P < 0.001, see **Fig. 1K**); and that of LAMP1, LAMP2 and BECN1 with 24 h of fasting, as compared with nonfasted diluent-treated controls (**Fig. 10G–J**), indicating accumulation of these proteins with inhibition of lysosome acidification during fasting. Taken together with the transcriptional upregulation of their cognate genes with 24 h of fasting, the lack of a commensurate increase in the abundance of these autophagy-lysosome proteins in the myocardium (as compared with nonfasted controls), implies ongoing consumption of the autophagy-lysosome machinery components with fasting-induced upregulation of autophagic flux (see **Figs. 1J–M** and **2D and E**).

Fasting stimulates activation of TFEB in the myocardium

Recent studies have uncovered a potential mechanism for transcriptional replenishment of the autophagy-lysosome machinery with starvation; and ascribed a central role to the rapid starvation-induced dephosphorylation and cytoplasm to nuclear translocation of TFEB (transcription factor EB),[45-48] a basic helix-loop-helix transcription factor of the MiTF family, with resultant upregulation of its target genes.[47,49,50] Of note, TFEB is unique in coordinately upregulating the autophagy-lysosome machinery,[47] and is expressed in the adult mammalian myocardium.[51] We examined whether fasting, in vivo, is a stimulus for activation of TFEB in the myocardium. Given a lack of consensus on the suitability of the available antibodies in identifying the endogenous TFEB protein,[46,48,52] we first evaluated the specificity of a polyclonal anti-TFEB antibody employed in recent publications to detect endogenous human TFEB;[46] which is predicted to detect murine TFEB based on sequence similarity within the epitope employed in its generation; in a murine atrial myocyte cell line (HL-1 myocytes) and mouse hearts (**Fig. S7**). The

Figure 5 (See previous page). Intermittent fasting provokes worsening cardiomyopathy in *lamp2* null mice. (**A**) Representative 2D-directed M mode echocardiographic images ± from *lamp2* null mice and littermate wild-type (WT) mice subjected to intermittent fasting, or provided ad libitum access to food for 5 wk, on a fed day. (**B–E**) Serial echocardiographic evaluation of LVEDD (left ventricular end-diastolic diameter; **B**), % fractional shortening (**C**), left ventricular mass (LVM) (**D**) and body weight (**E**) in male *lamp2* null (*black squares and dotted line*) and littermate wild-type males (*open circles and solid line*) subjected to intermittent fasting (IF); N = 5 to 7/group. '*' indicates P < 0.05 for *lamp2* null vs. wild type by post-hoc test after 2-way ANOVA.
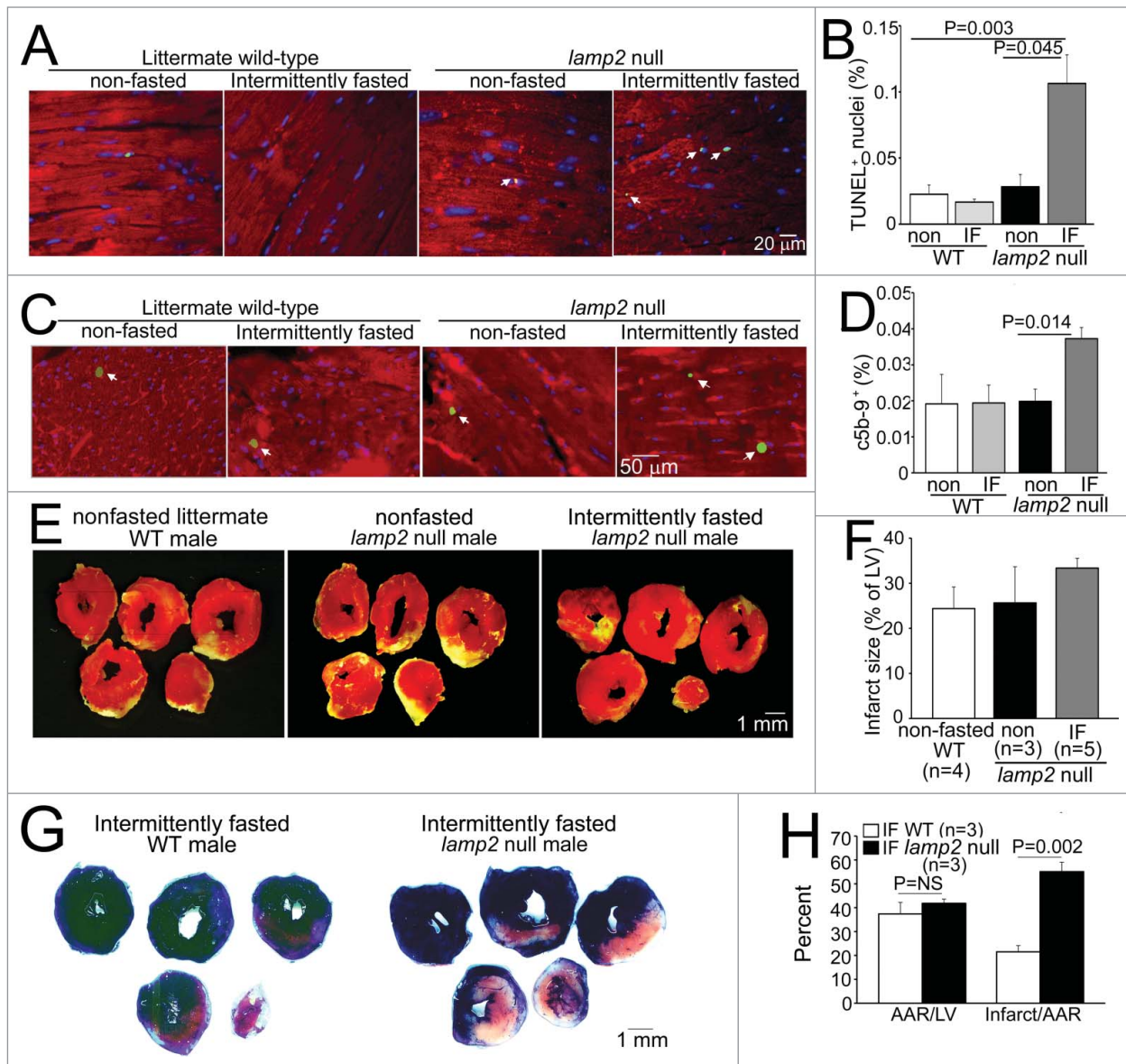
Figure 6. Intermittent fasting provokes cardiomyocyte death in *lamp2* null mice and loss of cardioprotection to ischemia-reperfusion injury. (**A and B**) Representative images of TUNEL-labeled cardiomyocyte nuclei (green, *arrowheads*; **A**) with quantification of TUNEL-positive nuclei (blue, DAPI) as percent of total (**B**; N = 3 to 5 mice/group) in *lamp2* null mice or littermate controls subjected to 5 wk of intermittent fasting (IF) or provided ad libitum access to standard chow. ACTA1 staining (red) was employed to delineate cardiomyocytes. *P* value is by post-hoc analysis after one-way ANOVA. (**C and D**) Representative images of c5b-9-labeled cardiomyocyte nuclei (green, *arrowheads*; **C**) with quantification of C5-C9-positive nuclei (blue, DAPI) as percent of total (**D**; N = 3 or 4 mice/group) in mice treated as in (**A**). ACTA1 staining (red) was employed to delineate cardiomyocytes. P value is by post-hoc analysis after one-way ANOVA. (**E and F**) Representative images of TTC-stained sections of hearts (**E**) and infarct size (at 24 h; **F**) after in-vivo LAD territory ischemia (30 min) followed by reperfusion, in *lamp2* null mice subjected to intermittent fasting for 5 wk (with surgical modeling on a fed day), nonfasted *lamp2* null mice and littermate controls. (**G and H**) Representative images of TTC and Evans blue-stained sections of hearts subjected to ischemia-reperfusion injury (**G**) on a fed day after 5 wk of intermittent fasting in *lamp2* null mice or wild-type controls, with quantification of area-at-risk and infarct size (**H**). *P* value is by *t* test. LV, left ventricle.

antibody detected a band migrating between molecular mass markers of 50 kDa and 75 kDa in the nuclear fraction (labeled as 2; **Fig. 11A and B**), which likely corresponds to murine TFEB protein encoded by transcript variants 2 and 3 (NP_001155194.1, see **Fig. S7** for controls); along with 2 other prominent bands close to these molecular mass standards (labeled as 1 and 3, **Fig. 11A**), which could represent the alternative isoform (NP_035679.3) or posttranslationally modified forms of the protein. To determine whether fasting activates TFEB with cytoplasm to nuclear translocation, in vivo (mirroring the observations in vitro),[45,46,48] we examined the relative abundance of endogenous TFEB in nuclear and cytoplasmic fractions of

myocardial extracts from fasted and control mice. Fasting for 24 h resulted in marked accumulation of TFEB protein in the nuclear subfraction, with a rapid decline observed after refeeding (**Fig. 11A and B**). This closely tracks the observed transcriptional changes of the candidate autophagy-lysosome genes (**Fig. 8**), which are all putative TFEB targets.[47,49,50] Commensurate with the observation that TFEB autoregulates its expression,[53] transcript levels for *Tfeb* gene also increased and declined significantly with a fasting-refeeding cycle, as compared with respective controls (**Fig. 11C**). These data suggest a prominent role for TFEB in coordinating the transcriptional response to replenish the lysosomal degradative machinery, with fasting, in the myocardium, in vivo. Interestingly, *Tfeb* transcripts were significantly upregulated after 3 wk of intermittent fasting, on a fed day (**Fig. 11C**), suggesting a possible role for enhanced TFEB activity in transducing the cardioprotective effects of intermittent fasting. Taken together, these data indicate that TFEB activation and transcriptional upregulation may mechanistically drive the cyclical transcriptional induction of the lysosomal degradative machinery with each fasting-refeeding cycle, facilitating beneficial autophagy.
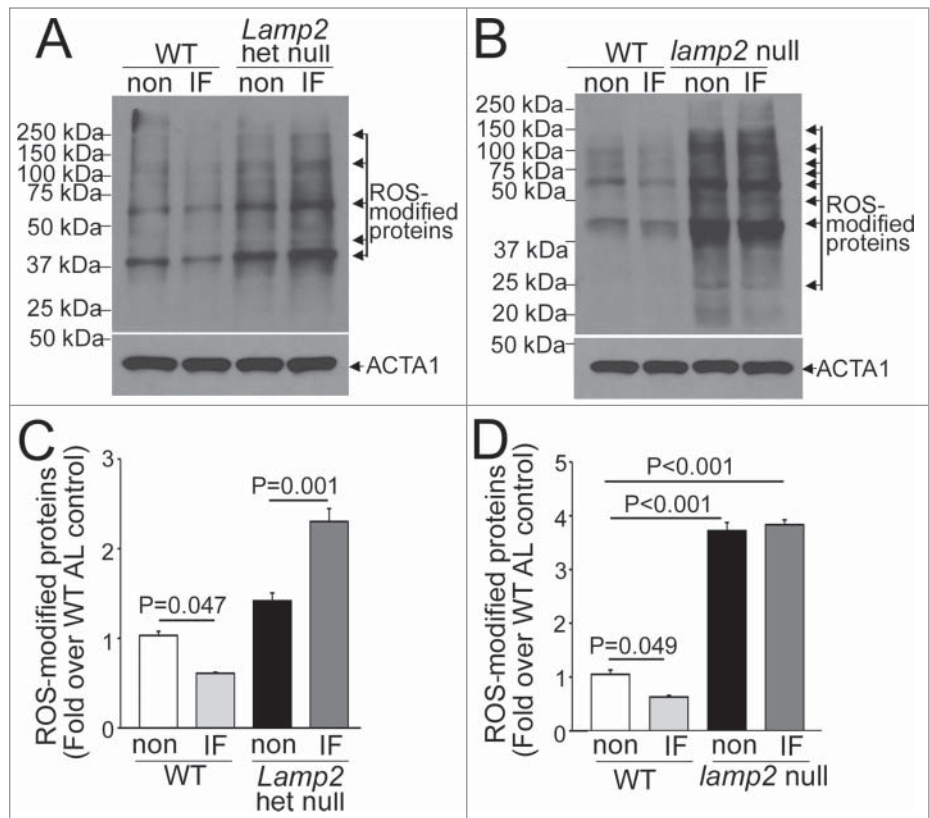

Figure 7. Intermittent fasting (IF) modulates myocardial ROS levels. (**A and B**) Representative immunoblot demonstrating abundance of ROS-modified (carbonylated) proteins in cardiac extracts from *Lamp2* heterozygous null (**A**) and *lamp2* null mice (**B**), together with respective wild-type controls, on a fed day after intermittent fasting or in nonfasted ad libitum fed controls (non). (**C and D**) Quantification of prominent bands (marked with arrows) from immunoblots in (**A and B**), respectively. N = 3 /group. *P* is by post-hoc analysis after one-way ANOVA.

Endogenous TFEB-mediated stimulation of autophagic flux is essential for cytoprotective effects of repetitive starvation on hypoxia-reoxygenation injury

Given that our in vivo observations suggest that fasting induced activation of TFEB and up regulation of autophagic flux may transduce the beneficial effects of intermittent fasting, we examined whether repetitive starvation preconditions NRCMs to protect against hypoxia-reoxygenation (HR) injury, via endogenous TFEB (see schematic in **Fig. S1B**). Starvation in NRCMs transcriptionally upregulated TFEB expression, indicating its activation, as observed in multiple other cell types,[45,46,48,53] in a manner dependent upon endogenous TFEB (**Fig. 12A**). Importantly, knockdown of endogenous TFEB prevented starvation-induced upregulation of autophagic flux, assessed as the ratio of LC3-II (**Fig. 12B and C**) and SQSTM1 (**Fig. 12B and D**) in the presence of bafilomycin A$_1$ (to inhibit lysosomal processing) versus diluent. We next determined whether repetitive starvation would offer cytoprotection to HR-induced cell death.[36] Interestingly, 2 cycles of repetitive starvation were associated with a modest (and statistically significant) ~13% to 15% reduction in HR-induced cell death (**Fig. 12E and F**). Knockdown of endogenous TFEB also increased HR-induced cell death and completely prevented the cytoprotective effects of preceding repetitive starvation stimuli (**Fig. 12E**). Importantly, the autophagy-lysosome machinery played a critical role in this observation, as the cytoprotection against HR-induced cell death was also lost with concomitant knockdown of LAMP2 to prevent autophagosome processing (as in **Fig. 8B**) or BECN1 to prevent autophagosome formation (as in **Fig. 8A**; see **Fig. 12F**). These data indicate that endogenous TFEB is essential for enhancement of autophagic flux with fasting, which transduces the preconditioning effect of repetitive starvation in cardiac myocytes.

Intermittent fasting stimulates cellular degradative pathways

The benefits of intermittent fasting (or repetitive starvation) on cytoprotection against ischemia-reperfusion (or hypoxia-reoxygenation) are observed in a fed state, while autophagic flux is not upregulated above the basal state. These benefits are not accrued if lysosome function is impaired with heterozygous knockout of *Lamp2* or its ablation, in vivo (or knockdown of a master regulator of lysosome function, TFEB, in vitro), resulting in impairment of autophagic flux and accumulation of damaged mitochondria (**Figs. 2G and 4G**) and upregulation of myocardial oxidative stress (**Fig. 7**) on a fed day. It is conceivable that other lysosomal

pathways are mechanistically involved in concert with, or independently of autophagy, in transducing the observed preconditioning effects. To explore potential alternative mechanisms, we examined the myocardial gene expression changes on a fed day in wild-type mice after intermittent fasting, and compared them with similarly modeled *lamp2* null mice (as in **Figs. 4D–G**, **5**, and **6**; **Fig. S4**); at a time point immediately predating the observed benefits on cardioprotection at 6 wk after the intermittent fasting regimen (as in **Fig. 1D–G**; **Fig. 3A–D**). Nonfasted age-matched *Lamp2* null and wild type were studied in parallel, in a 2-by-2 design, as controls.

Changes in gene expression with intermittent fasting (vs. nonfasted controls) were uniform within each genotype (wild-type and *lamp2* null mice) but markedly divergent between the 2 (**Fig. 13A**), providing an opportunity to dissect the intermittent fasting-induced changes observed only in the wild type mice, but not with concomitant lysosomal dysfunction in *lamp2* null mice (**Fig. 12B** and **Table S1**; see the nonoverlapping set of 1584 genes). Analysis of functional pathways revealed
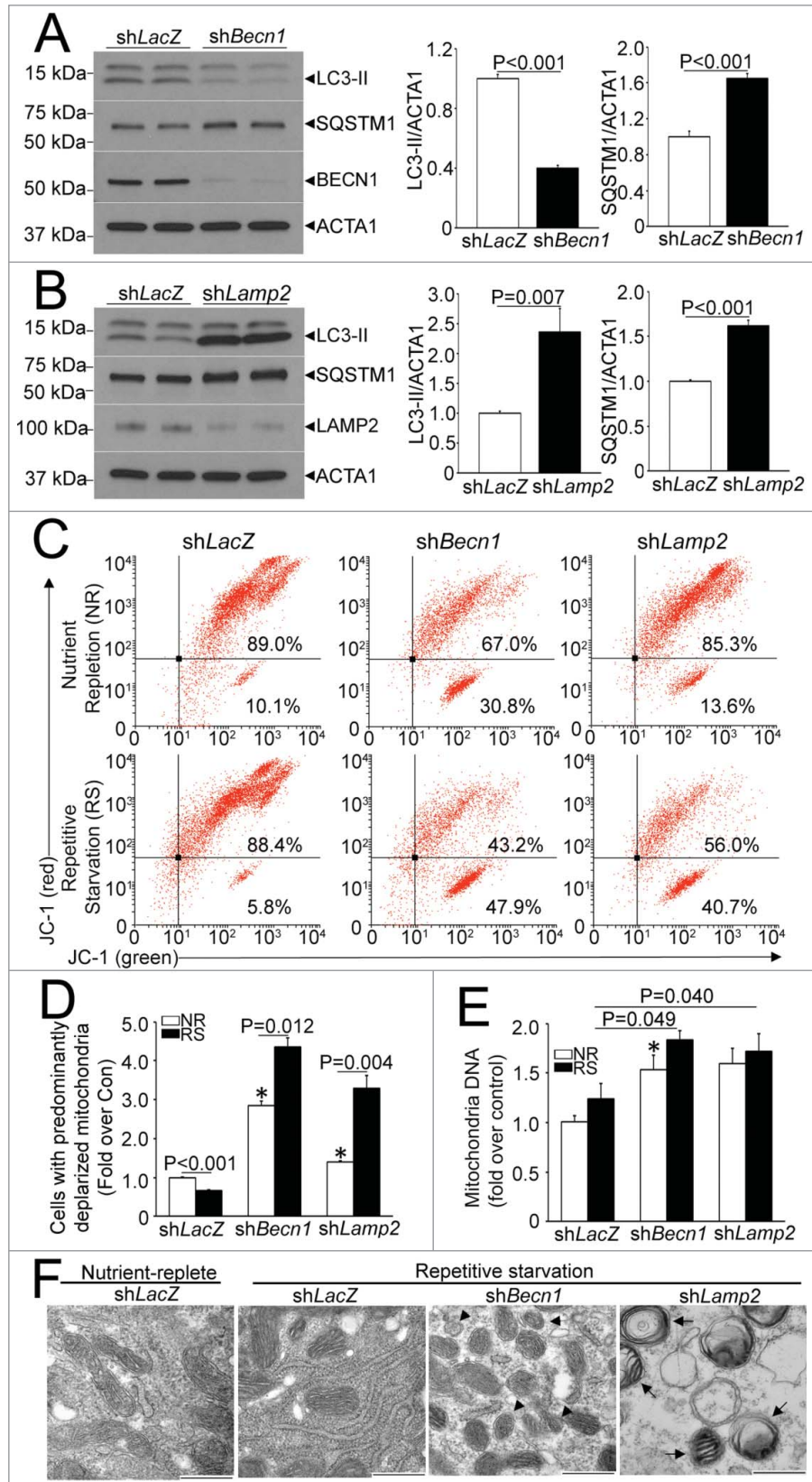

Figure 8. Repetitive starvation-induced autophagy controls mitochondrial quality. (**A**) Representative immunoblot (*left*) and quantification of LC3-II (*middle*) and SQSTM1 (*right*) 12 h in the presence of sh*Becn1* or sh*LacZ* as control (all at multiplicity of infection [MOI] = 10). N = 4/group. *P* values shown are by t test. (**B**) Representative immunoblot (*left*) and quantification of LC3-II (*middle*) and SQSTM1 (*right*) 12 h in the presence of sh*Lamp2* or sh*LacZ* as control (all at MOI = 10). N = 4 /group. *P* values shown are by t test. (**C**) Representative flow cytometric analyses of JC-1 expression in NRCMs subjected to 2 12-h cycles of starvation interspersed with 12 h periods of culture in a nutrient replete medium; or provided continual access to nutrients (as depicted in Fig. S1B), in the presence of sh*Becn1* (as in **A**), sh*Lamp2* (as in **B**) and sh*LacZ* as control. (**D**) Quantification of cells expressing predominantly depolarized mitochondria (right lower quadrant; N = 4 /group. *P* values shown are by post-hoc test after one-way ANOVA. (**E**) Mitochondrial DNA content in cells treated as in A. N = 6 /group. *P* values shown are by post-hoc test after one-way ANOVA. For (**D and E**) * indicates *P* < 0.05 vs. sh*LacZ*, nutrient replete group; NR, nutrient replete; RS, repetitive starvation. (**F**) Representative transmission electron micrographs demonstrating mitochondrial ultrastructure in NRCMs treated with sh*Lamp2*, sh*Becn1* or sh*LacZ* as control and subjected to repetitive starvation as in (**A**), or cultured in nutrient-replete medium in the presence of sh*LacZ* as control. Mitochondrial ultrastructure appears normal in sh*LacZ* cells subjected to nutrient replete and repetitive starvation conditions, whereas mitochondria appear fragmented with sh*Becn1* (arrowheads) and within autophagosomes with sh*Lamp2* (arrows). Scale bar: 500 nm.
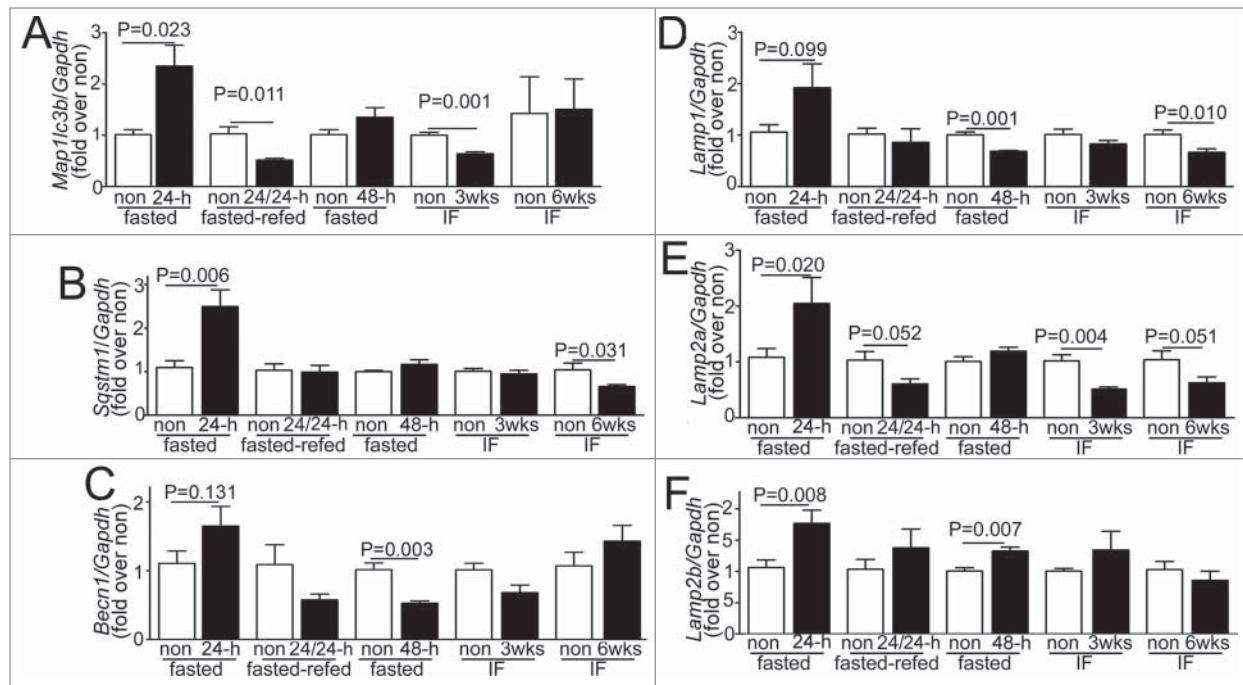
Figure 9. Fasting and refeeding result in transcriptional regulation of autophagy-lysosome machinery genes. (**A–F**) Quantitative PCR analysis of relative abundance of representative autophagy-lysosome machinery gene transcripts, namely *Map1lc3b* (coding for LC3B; **A**), *Sqstm1* (**B**), *Becn1* (**C**), *Lamp1* (**D**), *Lamp2a* (**E**) and *Lamp2b* (**F**) in adult male C57BL/6 mice subjected to 24 h of fasting, fasting for 24 h followed by refeeding for 24 h (fasted-refed), 48 h of fasting; and intermittent fasting for 3 and 6 wk (with samples procured on a fed day). Age-matched nonfasted controls were employed for each group. Control RNA for comparing the 24- and 48-h fasted RNA was prepared from the same nonfasted mouse hearts, and ran separately with each experimental group. N = 4 to 8/group. *P* value is by *t* test versus respective controls.

major changes in genes governing transcription and metabolism (**Fig. 13C**; also see list of genes separated by genotype in supplementary data), with upregulation of intracellular degradative and metabolic processes; and downregulation of cell death pathways (**Table 4**) as likely mechanisms for the observed cardioprotective effects of intermittent fasting. Taken together with the effects of intermittent fasting on autophagy, these data raise the intriguing hypothesis that global regulation of lysosome function with intermittent fasting is mechanistically involved in preconditioning the myocardium via effects on organelle quality, metabolism, and cell death.

Discussion

Calorie restriction and stimulation of autophagy have salutary effects on life-span extension and cardioprotection. Our study indicates a central role for transcriptional stimulation of the autophagy-lysosome machinery in intermittent fasting-induced protection against ischemia-reperfusion injury based on the following observations. First, intermittent fasting preconditions the myocardium with a ~50% reduction in infarct size with experimental ischemia-reperfusion injury in both sexes; and this benefit is lost in *Lamp2* heterozygous null mice, wherein lysosomal function and consequently autophagy are impaired, principally under stress. Second, intermittent fasting stimulates autophagosome

accumulation in the setting of lysosomal dysfunction, which provokes adverse ventricular remodeling and heart failure in *lamp2* null mice, wherein basal autophagic flux is impaired. Third, intermittent fasting transcriptionally stimulates the autophagy-lysosomal machinery in a cyclical fashion to keep the machinery primed with repetitive cycles of fasting-induced autophagy; associated with nuclear translocation of transcription factor EB, which is a master regulator that coordinates the biogenesis of autophagy-lysosome machinery. Fourth, endogenous TFEB plays a critical role in enhancement of autophagic flux and starvation-induced cytoprotection to hypoxia-reoxygenation injury, in cardiac myocytes, in vitro. Last, intermittent fasting attenuates myocardial oxidative stress and transcriptionally reprograms the myocardium, even on a fed day, to stimulate degradative processes and suppress cell death pathways, likely contributing to the observed beneficial effects.

Previous studies have described multiple salutary effects of intermittent fasting on life-span prolongation in *C. elegans*[54] and rodents;[22,55] reduction in infarct size with improved mortality and attenuation of postinfarction remodeling in the heart;[23,24] improved glucose regulation and attenuation of hypoxic insult in neurons[25] in experimental models; and remarkable effects on weight loss and improved glucose-regulation in obese women.[21] Our study extends these observations by defining the need for an optimal frequency and duration of the fasting regimen to derive the cardioprotective effects; and suggests the hypothesis that
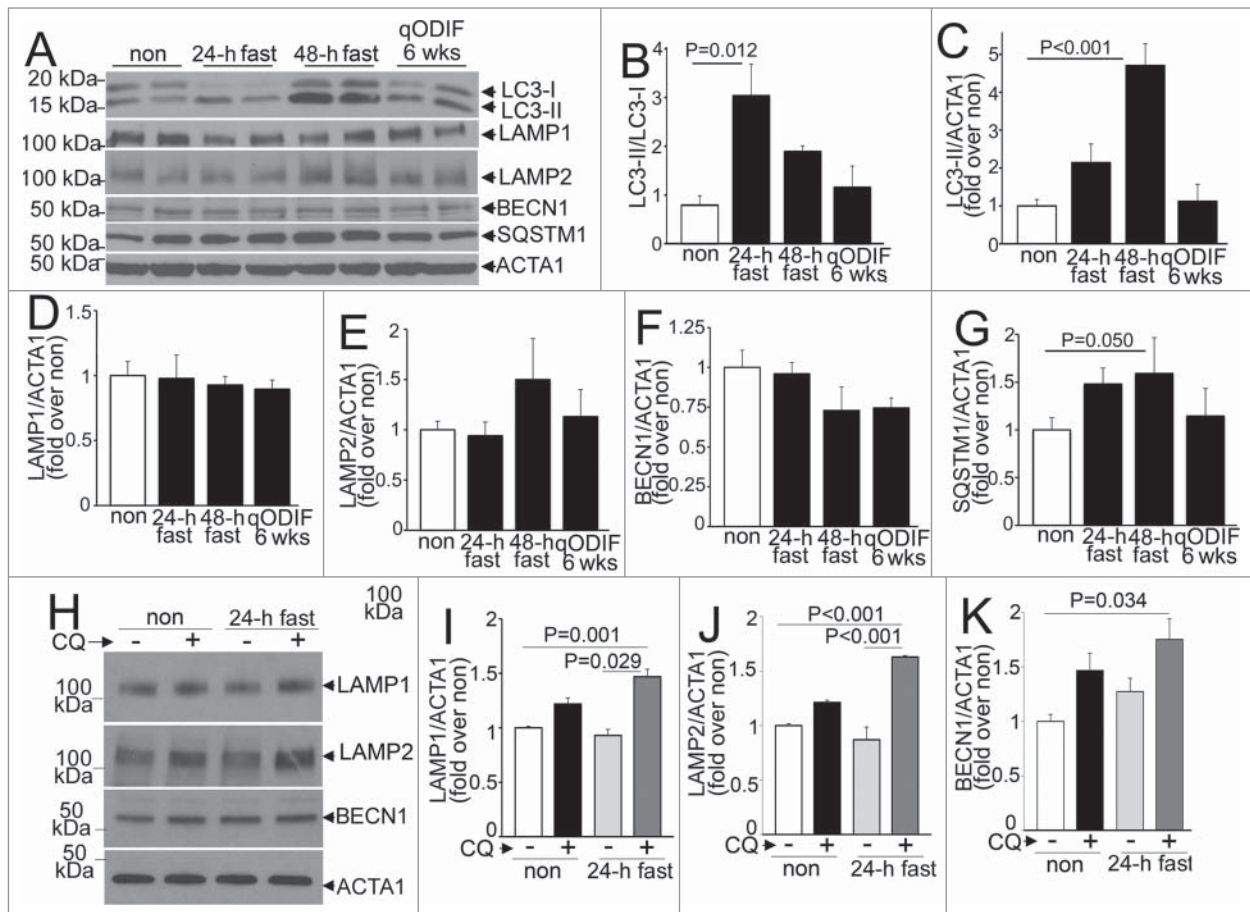
Figure 10. Intermittent fasting induces autophagy without depletion of myocardial autophagy-lysosome machinery proteins. (**A–G**) Representative immunoblots (**A**) and quantification of LC3 processing (ratio of LC3-II to LC3-I; **B**); and abundance of total LC3 (**C**), LAMP1 (**D**), LAMP2 (**E**), BECN1 (**F**) and SQSTM1 (**G**) in C57BL/6 male mice subjected to fasting for 24 h, 48 h and intermittently fasted for 6 wk (with samples procured on a nonfasted day) as compared with nonfasted controls. N = 4 /group. P value is by post-hoc test after one-way ANOVA. ACTA1 was employed as loading control. (**H–K**) Representative immunoblot (**H**) and quantification of LAMP1 (**I**), LAMP2 (**J**) and BECN1 (**K**) in myocardial extracts from wild-type mice treated with CQ or diluent, concomitantly with 24 h of fasting or with ad libitum feeding (also see **Fig. 1K**). N = 3 /group. P values are by post-hoc test after one-way ANOVA.

frequency and duration of fasting episodes have additive benefits that accumulate with continuation of an intermittent fasting regimen. These observations are particularly relevant, as while sustained calorie restriction has well-established effects on preventing cardiovascular disease and aging,[3,4] and confers cardioprotection to ischemia-reperfusion injury.[56] Clinical studies have repeatedly demonstrated an inability to maintain sustained calorie restriction for prolonged periods in obese subjects,[57,58] who are at markedly elevated risk for development of cardiovascular disease. Conversely, intermittent fasting is routinely practiced by diverse human social groups for religious and/or cultural reasons. Early clinical studies suggest excellent short-term efficacy in treating obesity and its attendant metabolic risks,[21] improving glucose regulation and favorably altering the cardiovascular risk profile (reviewed in ref.),[59] thus making it an attractive alternative that needs to be evaluated for deriving benefits of calorie restriction.

Our study implicates an essential role for normal lysosomal function, particularly with relevance to efficient execution of macroautophagy; and hints at a prominent role of

TFEB-mediated transcriptional replenishment of the autophagy-lysosome machinery in transducing the beneficial effects of intermittent fasting. It is important to note that other mechanisms may contribute to the observed benefits, too. In this regard, we have examined the role of CMA. Our data do not suggest an accumulation of CMA substrates,[40] as would be expected with ablation of the LAMP2A isoform in *lamp2* null mice),[28] which could conceivably be due to upregulation of alternate protein degradation mechanisms. Importantly, the levels of these substrates were not altered by the intermittent fasting regimen, suggesting that CMA is unlikely to be a significant contributor to the observed cardioprotective effects. In contrast, we observed accumulation of abnormal mitochondria, which are substrates for macroautophagy and increased oxidative stress in LAMP2 deficient mice on a fed day, paralleling impairment in macroautophagy, which is the major pathway for removal of damaged mitochondria.[60] LAMP2, together with LAMP1, plays an important role in cholesterol efflux,[61] which also may be mechanistically important in the observed benefits of intermittent fasting,
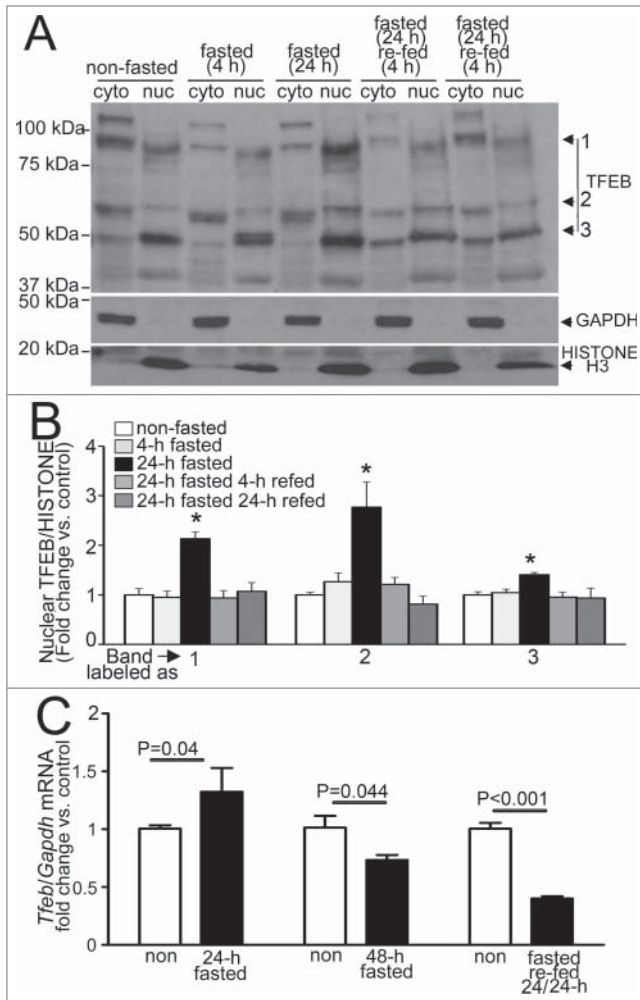
Figure 11. Fasting induces nuclear translocation of TFEB in the myocardium. (**A and B**) Representative immunoblot (**A**) with quantification of nuclear TFEB (**B**, bands numbers from **A**) in nuclear and cytoplasmic subfractions from wild-type adult male C57BL/6 mouse hearts subjected to indicated durations of fasting and refeeding. Immunoblotting for GAPDH and Histone H3 was employed to detect enrichment of cytoplasmic and nuclear subfractions, respectively. N = 3 /group. P value is by post-hoc analysis after one-way ANOVA. (**C**) Quantitative PCR analysis of relative abundance of *Tfeb* transcript in mice subjected to 24 or 48 h of fasting (with age matched nonfasted controls); fasting for 24 h followed by refeeding for 24 h (fasted-refed). N = 4 to 8/group. *P* value is by t test vs. control. RNA from a common group of nonfasted mice was employed as control to compare transcript abundance in 24- and 48-h fasted samples.

and needs to be explored further. In addition, we did not observe any obvious effect of intermittent fasting or LAMP2 ablation on microautophagy[62] in the ultrastructural studies, but definitive studies on its role will require development of tools to modulate this pathway.

We observe that autophagic flux is not upregulated above basal levels on a fed day after intermittent fasting (or in culture in nutrient replete medium after starvation, in vitro), at a time when the benefits of cytoprotection are observed. This suggests that the preconditioning effect of the lysosomal degradative pathways on maintenance of mitochondrial quality (as demonstrated

by our data in **Figs. 2G and 4G**),[19] and perhaps on maintenance of ER homeostasis[63] plays a central role in shoring up cellular defenses to withstand the stress.[64] Indeed, we observe a reduction in prevalence of depolarized mitochondria in repetitively starved cardiomyocytes, in vitro (**Fig. 8**) and reduced abundance of carbonylated proteins in the myocardium of intermittently fasted mice on a fed day (**Fig. 7**), suggesting that intermittent fasting stimulates lysosome function to remove damaged organelles that are the source for deleterious ROS generation,[38,64] as a mechanism for preconditioning the myocardium to ischemia-reperfusion injury.[39] Additional upstream signaling events that link fasting to stimulation of lysosomal pathways, including autophagy, may also participate in preconditioning responses. Fasting-induced activation of AMPK and suppression of MTOR signaling, are 2 candidate pathways that have been previously demonstrated to have no effect (as with AMPK[65]) or facilitate ischemic preconditioining (as with rapamycin-mediated inhibiton of MTOR[66]) in the myocardium. Fasting-induced upregulation of SIRT/sirtuin signaling and protein deacetylation are also implicated in provoking myocardial autophagy;[11] and future studies are required to determine the role of these signaling pathways in intermittent fasting-induced cardioprotection.

Interestingly, we observe nuclear translocation of TFEB with fasting in the myocardium; paralleling the observations with starvation in various noncardiomyocyte cell types, in vitro.[45-47,50] It is therefore conceivable that the mechanism for TFEB activation with fasting, in vivo, is similar to that observed in vitro, with starvation-induced MTOR inhibition resulting in dephosphorylation and nuclear translocation of TFEB. However, while both fasting and starvation induce autophagy, it is likely that fasting is sensed as a metabolic shift in the myocardium, unlike total nutrient deprivation employed in the in vitro modeling of starvation; which points to the need for elucidating unique signaling pathways that drive TFEB activation with fasting, in vivo. Our findings suggest a critical role for TFEB in transducing starvation-induced upregulation of autophagic flux, in vitro. In this context, given that germline ablation of TFEB results in embryonic lethality,[67] generation of conditional cardiomyocyte TFEB knockout mice will be required to confirm its critical role in fasting-induced cardioprotection, in vivo.

Our data suggest the hypothesis that the transcriptional replenishment of the autophagy-lysosome machinery by fasting (and starvation as previously described) may be a critical determinant of beneficial autophagy; which permits living organisms to survive what is likely to have been one of the earliest evolutionary stresses accompanying the origin of life. Indeed, we have previously found that transcriptional suppression of the autophagy machinery with reperfusion-induced accumulation of BECN1 explains the lack of a protective role of the observed extent of autophagy induction in cardiac ischemia-reperfusion injury.[36,68] Further insights into this process could be gleaned via careful examination of the effects of intermittent fasting on the transcriptional program of the injured myocardium, in future studies.

In summary, our data implicate a central role for lysosomal degradative pathways in facilitating the previously described cardioprotective effects of intermittent fasting. Observations made
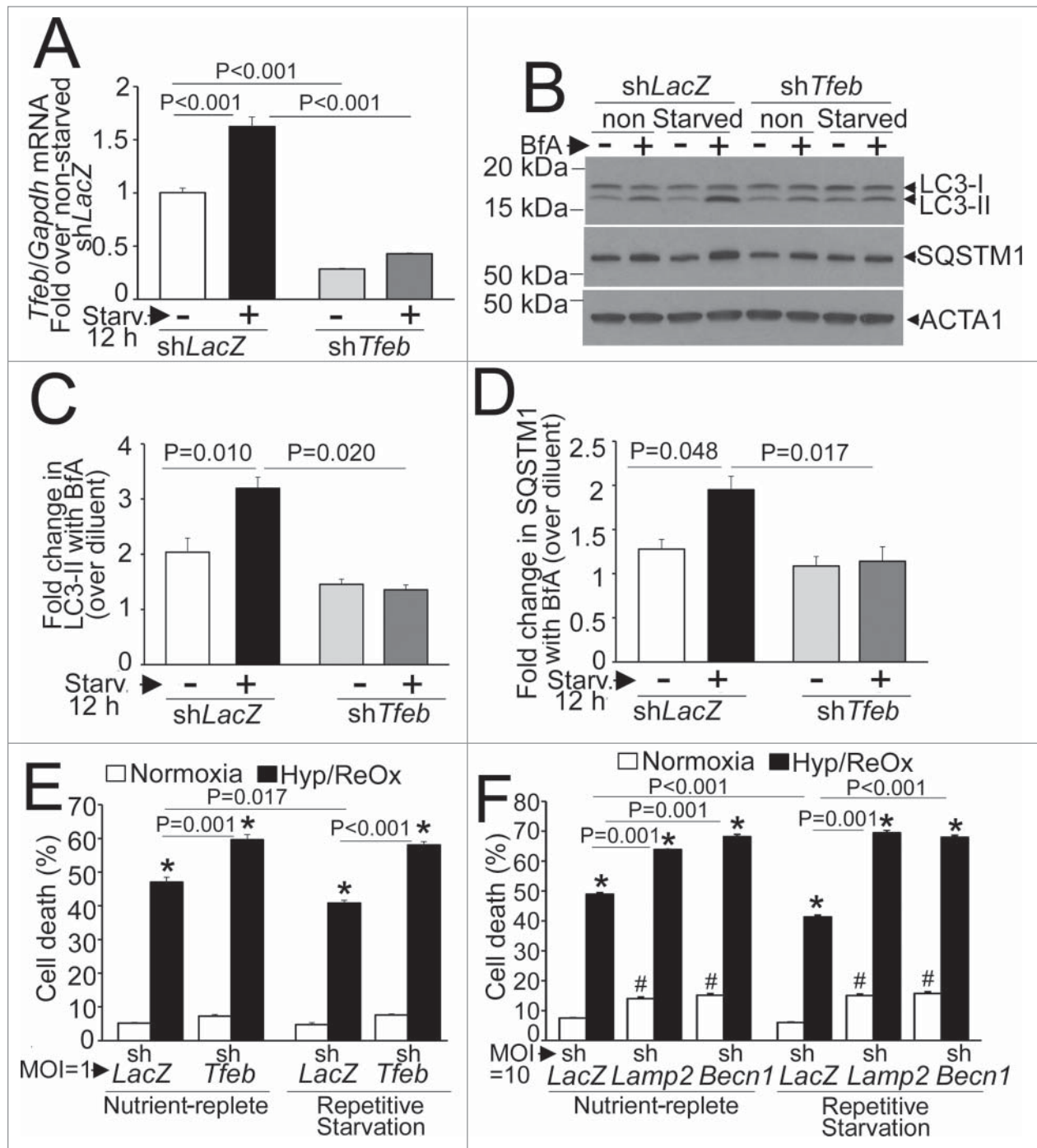
Figure 12. Endogenous TFEB is essential for starvation-induced upregulation of autophagic flux and its cytoprotective preconditioning effect on hypoxia-reoxygenation injury in NRCMs. (**A**) *Tfeb* transcripts in NRCMs adenovirally transduced with shRNA targeting rat *Tfeb* (or sh*LacZ* as control, both at MOI = 1 for 60 h) and subjected to starvation (or cultured in nutrient-rich medium) for 12 h. N = 3 /group. *P* value is by post-hoc test after one-way ANOVA. (**B–D**) Representative immunoblot (**B**) with quantification of LC3-II (**C**) and SQSTM1 (**D**) in NRCMs adenovirally transduced with shRNA targeting rat *Tfeb* (or sh*LacZ* as control, both at MOI = 1 for 60 h) and subjected to starvation (or cultured in nutrient rich medium) for 12 h, in the presence of bafilomycin A_1 (or diluent) to inhibit lysosomal acidification. N = 3 /group. *P* value is by post-hoc test after one-way ANOVA. (**E**) Cell death in NRCMs adenovirally transduced with shRNA targeting rat *Tfeb* (or sh*LacZ* as control, all at MOI = 1) and subjected to 2 12-h periods of starvation interspersed to 12 h periods of feeding, followed by exposure to hypoxia (6 h) and reoxygenation (18 h) after the final 12 h of feeding, to simulate repetitive fasting conditions, in vitro (schematic in Figure S1B). (**F**) Cell death in NRCMs adenovirally transduced with shRNA targeting rat *Becn1* or *Lamp2* (or sh*LacZ* as control, all at MOI = 10) and treated as in (**E**). N = 14 to 16/group; and *P* values are by post-hoc test after 2-way ANOVA for E, F. '*' indicates *P* < 0.05 vs. respective normoxia group; and '#' indicates *P* < 0.05 vs. respective sh*LacZ*-treated group within normoxic nutrient replete and repetitive starvation conditions.
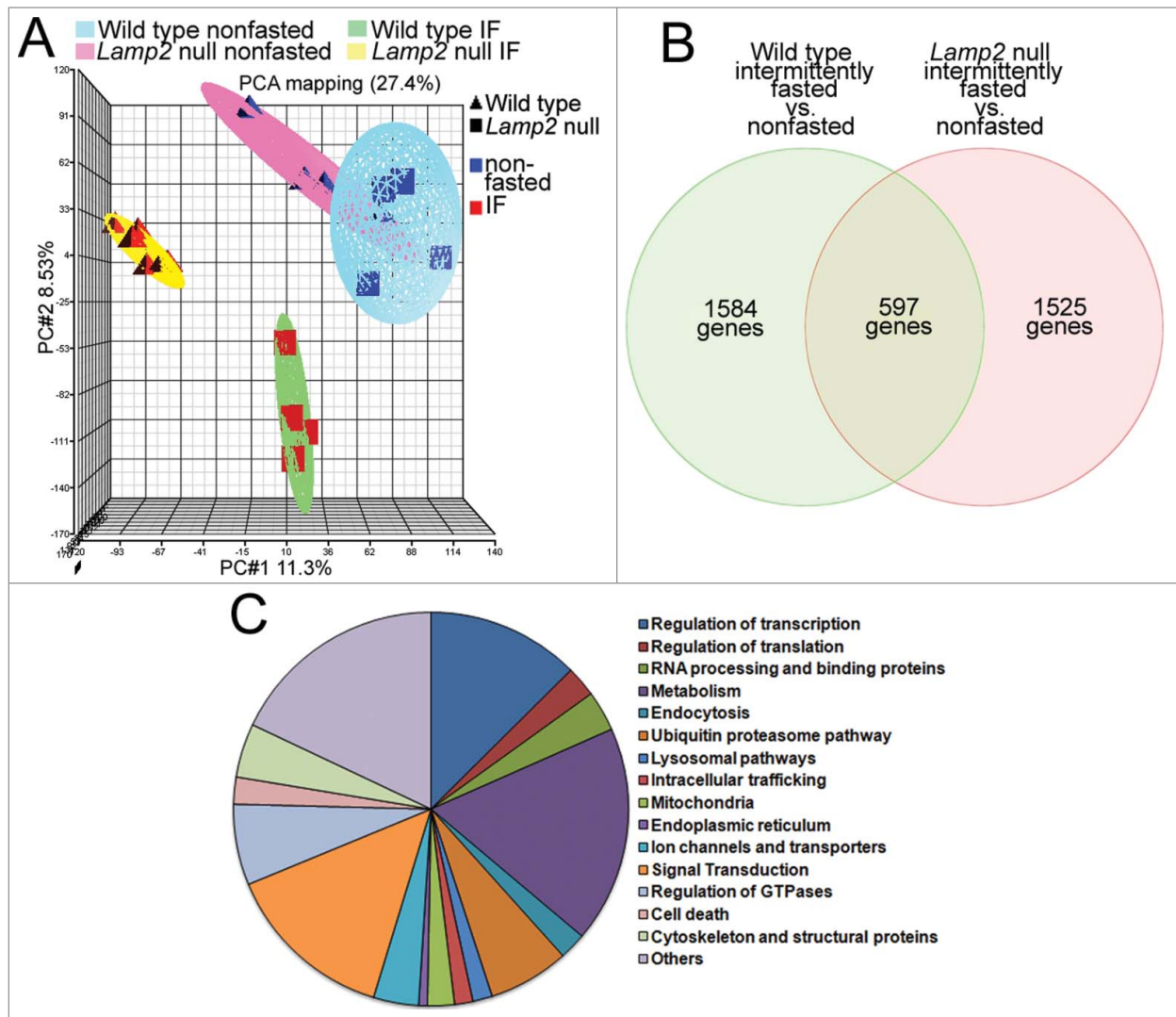
Figure 13. Intermittent fasting (IF) transcriptionally regulates cellular degradative, metabolic pathways, and cell death pathways. (**A**) Principal component analysis demonstrating markedly divergent regulation of gene transcription in hearts from *lamp2* null and littermate male wild-type mice subjected to intermittent fasting or provided ad libitum access to standard chow (as in **Fig. 3B–E**); n = 4 to 6/group. IF stands for intermittent fasting. (**B**) Venn diagram depicting distribution of differentially regulated genes in wild-type and *lamp2* null male mice, as compared with respective age-matched nonfasted controls, as in (**A**). (**C**) Pie chart depicting relative distribution of genes by function in intermittently fasted mice (as compared with nonfasted mice) specifically in the subset that does not overlap with genes differentially regulated in similarly treated *lamp2* null mice (as in **B**).

herein also point to the need for exploring the transcriptional regulation of the cytoprotective lysosomal pathways to foster development of translational strategies to derive the benefits of calorie restriction in promoting cardiovascular health.

Materials and Methods

Studies with mice

Wild-type mice of the C57BL/6 strain were obtained from Jackson Laboratories. Mice with cardiomyocyte-specific expression of GFP tagged LC3 transgene[13] and those with *Lamp2* ablation[28] have been described before. Echocardiographic studies were performed as previously described in conscious mice.[69] All

animal studies were approved by the Animal Studies Committee at the Washington University School of Medicine and the Institutional Animal Care and Use Committee at the John Cochran VA Medical Center.

Intermittent fasting

Adult mice were housed in groups of up to n = 5 mice/cage and fed standard chow (Lab Diet, 5053; providing 3.4 Kcal/g with 62.1% Kcal derived from carbohydrates, 13.2% from fats, and 24.6% from protein) on a 6:00 PM to 6:00 AM night-day cycle, while housed on cedar pine chip bedding. Intermittent fasting was performed with total food deprivation and ad libitum access to water from 12:00 PM to 12:00 PM of the following day to implement alternate periods of 24 h fasting and feeding, with

Table 4. List of top 15 GO (Gene Ontology) pathways selectively up- and downregulated only in wild-type mice subjected to intermittent fasting (vs. nonfasted controls) on a fed day

Pathway	P value	Number of genes	Fold enrichment
Upregulated genes			
Proteolysis (GO:0006508)	0.015	40	1.46
Cellular macromolecule catabolic process (GO:0044265)	0.011	27	1.67
Macromolecule catabolic process (GO:0009057)	0.024	27	1.55
Modification-dependent protein catabolic process (GO:0019941)	0.002	26	1.93
Modification-dependent macromolecule catabolic process (GO:0043632)	0.002	26	1.93
Proteolysis involved in cellular protein catabolic process (GO:0051603)	0.004	26	1.83
Cellular protein catabolic process (GO:0044257)	0.004	26	1.82
Protein catabolic process (GO:0030163)	0.006	26	1.76
Oxidation reduction (GO:0055114)	0.081	25	1.40
Chromosome organization (GO:0051276)	0.011	20	1.86
DNA metabolic process (GO:0006259)	0.055	18	1.61
Chromatin organization (GO:0006325)	0.047	15	1.79
Translation (GO:0006412)	0.046	15	1.77
Regulation of cellular protein metabolic process (GO:0032268)	0.066	13	1.75
Cellular amino acid derivative metabolic process (GO:0006575)	0.004	11	2.94
Transmission of nerve impulse (GO:0019226)	0.077	11	1.83
Downregulated genes			
Cytoskeleton organization (GO:0007010)	1.67E-18	29	8.69
Ion transport (GO:0006811)	5.01E-17	38	5.21
Protein localization (GO:0008104)	5.00E-13	34	7.29
Intracellular signaling cascade (GO:0007242)	4.30E-12	36	3.40
Cation transport (GO:0006812)	9.88E-12	27	5.12
Metal ion transport (GO:0030001)	6.17E-10	23	5.08
Cell death (GO:0008219)	1.45E-9	24	4.62
Apoptosis (GO:0006915)	1.59E-9	23	4.83
Establishment of protein localization (GO:0045184)	1.91E-9	27	4.02
Programmed cell death (GO:0012501)	2.18E-9	23	4.18
Death (GO:0016265)	2.28E-9	24	4.52
Regulation of apoptosis (GO:0042981)	7.63E-9	24	4.24
Protein transport (GO:0015031)	7.79E-9	26	3.90
Regulation of programmed cell death (GO:0043067)	9.67E-9	27	4.18
Regulation of cell death (GO:0010941)	1.06E-8	24	4.16

change in bedding. Nonfasted control mice were simultaneously provided fresh food with change in bedding. Daily food intake per cage was weighed to calculate average daily food intake per mouse. Mice were weighed at weekly intervals on fed days. Terminal studies on mice were initiated between 8:00 to 10:00 AM after an overnight period of feeding (i.e., on a fed day).

Assessment of autophagic flux, in vivo

Mice subjected to various fastng regimens were injected with CQ (40 mg/kg intraperitoneally) 4 h prior to sacrifice to assess autophagic flux, in vivo, as previously described.[26]

Ischemia-reperfusion modeling

Mice were subjected to reversible left anterior descending artery ligation for 30 min followed by reperfusion, in an open-chest procedure, as described.[36] Overall surgical mortality was very low (<3 %). At 24 h post induction of ischemia, cardioplegic solution was injected retrogradely through the aorta in situ, followed by sectioning of the left ventricle in slices; which were incubated in triphenyl tetrazolium chloride for 30 min at 37°C. All surgeries were performed by one surgeon (C.J.W.) and uniform LAD ligation technique was confirmed by assessment of area at risk with injection of Evans Blue dye in separate cohort of

animals. For infarct size calculation, triphenyl tetrazolium chloride (TTC)-stained slices were imaged and infarct area quantified as non-TTC-stained (pale) area as a ratio of total myocardial area, as previously described.[70]

TUNEL and c5b-9 staining: Evaluation of cardiomyocyte TUNEL positivity and c5b-9 staining was performed, as previously described.[70,71]

Quantitative PCR analysis

Total RNA was extracted from mouse hearts using RNAeasy Fibrous Tissue Minikit (Qiagen). Quantitative PCR analysis was performed as described.[36] Primers employed were as follows: *Map1lc3b*: forward 5′- CGTCCTGGACAAGACCAAGT-3′, reverse 5′- ATTGCTGTCCCGAATGTCTC-3′[72] ; *Sqstm1*: forward 5′- GCTGCCCTATACCCACATCT-3′, reverse 5′-CGCCTTCATCCGAGAAAC-3′[73]; *Becn1*: forward 5′- AATCTAAGGAGTTGCCGTTATAC-3′ , reverse 5′-CCAGTGTC-TTCAATCTTGCC-3′[74]; *Lamp1*: forward 5′- ACATCAGCC-CAAATGACACA-3′, reverse 5′- GGCTAGAGCTGGCATTC ATC-3; *Lamp2a*: forward 5′- CCAAATTGGGATCCTAACCT-AA-3′, reverse 5′-TGGTCAAGCAGTGTTTATTAATTCC-3; *Lamp2b*: forward 5′- GGTGCTGGTCTTTCAGGCTTGATT-3′, reverse 5′- ACCACCCAATCTAAGAGCAGGACT-3[75];

Tfeb: forward 5′- GTCTAGCAGCCACCTGAACGT-3, reverse 5′-CAGGTCACAGCCTCCATGGT-3[76]; *Gapdh*: forward 5′-ACTCCCACTCTTCCACCTTC-3′, reverse 5′-TCTTGCTCA-GTGTCCTTGC-3′[75]; and *Rpl32*: forward 5′- CCTCTGGTG AAGCCCAAGATC-3′, reverse 5′- TCTGGGTTTCCGCCA-GTTT-3′.

Studies with NRCMs

Neonatal rat cardiac myocytes were isolated and cultured, as previously described.[77] Starvation was induced by culturing in serum-free HBSS (Invitrogen, 24020117). For assessment of mitochondrial polarization, NRCMs were incubated with JC-1 (10 mg/mL for 10 min) at 37°C in 5% CO_2, the cells were trypsinized and subjected to flow cytometry on FACScan instrument (Becton-Dickinson, NJ), as previously described.[68,78] Cyflogic software (CyFlo) was employed to analyze 20,000 events per run. Mitochondrial DNA content was assessed with quantitative PCR analysis as previously described.[68,78] Transmission electron microscopy was performed on NRCMs fixed in a modified Karnovsky's fixative, as previously described.[68,78] Hypoxia was induced by culturing cells in an oxygen control cabinet (Coy Laboratories, Grass Lake, MI) mounted within an incubator and equipped with oxygen sensor for continuous oxygen level monitoring. A mixture of 95% nitrogen and 5% CO2 was infused and oxygen levels in the chamber were monitored and maintained at <1%, as described.[36]

Generation of adenoviral constructs

Adenoviral particles for expression of shRNA targeting murine *Tfeb*, and a scrambled shRNA control were generated with BLOCKiT™ adenoviral system (Invitrogen, K4941–00). Specific oligo sequences employed were as follows: 1) shRNA targeting mouse *Tfeb* (with targeted coding sequence underlined) – top strand oligo: 5′-CACCGCGGCAGTACTATGACTAT-GATCGAAATCATAGTCATAGTACTGCCG-3′; bottom strand oligo: 5′- AAAACGGCAGTACTATGACTATGATT-TCGATCATAGTCATAGTACTGCCGC-3′.

Two) Scrambled shRNA as control to *Tfeb* shRNA- top strand oligo: 5′- CACCGGCGCTCATCGAATTAATAGTC-GAAACTATTAATTCGATGAGCGCC-3′; bottom strand oligo: 5′- AAAAAGGCGCTCATCGAATTAATAGTTTCGA-CTATTAATTCGATGAGCGCC-3′.

Adenoviral particles for shRNA targeting rat *Lamp2* were generated with the following oligos: top strand oligo: 5′-CACCGCCTTTAACCTGAAGGTGCACGAATGCACCTT-CAGGTTAAAGG-3′; bottom strand oligo: 5′-AAAAAGGCG CTCATCGAATTAATAGTTTCGACTATTAATTCGATGA-GCGCC-3′. Adenoviral particles for shRNA targeting *Becn1* (sh*Becn1*),[68] sh*LacZ* and exogenous expression of human TFEB have been previously described.[77]

Generation of conditional cardiac Tfeb transgenic mice

The coding sequence of mouse *Tfeb* (translated from transcript variant 2, NP_001155194.1, that encodes a protein similar in size to human TFEB) with a N-terminal FLAG tag was cloned into the α-Myosin Heavy Chain promoter –TetOMin construct generously provided by Jeffery Robbins, Cincinnati Children's Hospital. Resulting founders were mated with mice carrying the MYH6 promoter driven tTA transgene (also generously provided by Dr. Robbins); and pregnant and lactating mothers with pups were maintained on doxycycline-mixed chow (El-Mel diets, St. Charles, MO) until 8 wk of age. Myocardial extracts were prepared after 2 wk of being switched over to a standard chow diet in mice from founder line 4239, and employed as positive control for immunodetection of endogenous myocardial TFEB in mice.

Immunoblotting

Hearts were fractionated into nuclear enriched and cytoplasmic samples using CelLytic NuCLEAR Extraction kit (NXTRACT, Sigma); or crude extracts prepared followed by immunoblotting as described.[36] Antibodies employed were as follows: LAMP2, mouse monoclonal (Developmental Studies Hybridoma Bank, ABL-93), LAMP1 (Santa Cruz Biotechnology, sc-19992) and (Abcam, ab24170); anti-LC3 (encoding for MAP1LC3B subunit; Novus Biologicals, NB100–2220); SQSTM1 (Abcam, ab5416); BECN1/BECLIN-1 (Abcam, ab16998); TFEB (Bethyl Labs, A303–673A), LRRK2 (Cell Signaling Technology, 5559), NFKBIA/IκBα (Cell Signaling Technology, 4814), ALDOA/aldolase (Abcam, ab169544), GAPDH (Abcam, ab22555), and ACTA1/α-sarcomeric actin (Abcam, ab7799). ImageJ software was employed for quantitative analysis. Protein abundance was normalized to ACTA1 protein expression and reported as fold change vs. control.

Microarray analysis

Total RNA was extracted from mouse ventricles as above and hybridized to a Mouse Ref-6 Illumina BeadChip by the Genome Technology Access Center (GTAC) at Washington University School of Medicine and scanned with the BeadStation system from Illumina, Inc. Each chip was subjected to verification for quality standards for hybridization, labeling, staining, background signal, and basal level of housekeeping gene expression. After scanning the probe array, the resulting image was analyzed using the GenomeStudio software (Illumina), background was subtracted; and log transformation and quantile normalization were performed. Changes in gene expression were determined using Partek Genomics Suite on quantile-normalized and background-subtracted microarray data; and principal components analysis was performed. Significant gene lists were generated using an unadjusted P value <0.05 and fold change greater than 1.2 or less than −1.2. Functional analysis of pathways was performed using Database for Annotation Visualization and Integrated Discovery (DAVID).[79,80] List of genes were also annotated for functional significance based on Genecards (Weizmann Institute Database) and grouped under functional categories.

Assessment of myocardial ROS

ROS was monitored by detection of carbonylated proteins with Oxyblot™ Protein Oxidation Detection Kit (Chemicon/Millipore, S7150) following the manufacturer's instructions, as

described.[81] Briefly, 20 μg protein of cardiac extract was derivatized from carbonyl groups to a 2,4-dinitrophenylhydrazone (DNP) moiety with 1X 2,4-dinitrophenylhydrazine and denatured with SDS at the same time. After the protein was separated on a 12% precast gel (Bio-Rad, 456–1043) using standard SDS polyacrylamide electrophoresis under reducing conditions, the gels were transferred to a PVDF membrane and probed with primary rabbit anti-DNP and secondary goat anti-rabbit IgG (HRP-conjugated) antibodies provided in the kit and developed using enhanced chemiluminescence (Perkin Elmer, NEL103001EA). Then the DNP moiety is detected to measure the oxidative damage to a protein. Image J software was employed to quantify the relative abundance of carbonylated proteins.

Statistical analysis

Results are expressed as mean±SEM (unless otherwise specified). Statistical differences were assessed with the unpaired Student t test for 2 independent groups, one-way or 2-way ANOVA for comparing one or 2 variables, respectively, across multiple groups with SPSS software. The Bonferroni post-hoc test was employed after ANOVA for testing all pair-wise comparisons. A 2-tailed value of $P < 0.05$ was considered statistically significant.

Disclosure of Potential Conflicts of Interest

No potential conflicts of interest were disclosed.

Supplemental Material

Supplemental data for this article can be accessed on the publisher's website.

References

1. Schwartz LL, Kloner RA, Arai AE, Baines CP, Bolli R, Braunwald E, Downey J, Gibbons RJ, Gottlieb RA, Heusch G, et al. New horizons in cardioprotection: recommendations from the 2010 National Heart, Lung, and Blood Institute Workshop. Circulation 2011; 124:1172-9; PMID:21900096; http://dx.doi.org/10.1161/CIRCULATIONAHA.111.032698

2. Fontana L, Meyer TE, Klein S, Holloszy JO. Long-term calorie restriction is highly effective in reducing the risk for atherosclerosis in humans. Proc Natl Acad Sci USA 2004; 101:6659-63; PMID:15096581; http://dx.doi.org/10.1073/pnas.0308291101

3. Colman RJ, Anderson RM, Johnson SC, Kastman EK, Kosmatka KJ, Beasley TM, Allison DB, Cruzen C, Simmons HA, Kemnitz JW, et al. Caloric restriction delays disease onset and mortality in rhesus monkeys. Science 2009; 325:201-4; PMID:19590001; http://dx.doi.org/10.1126/science.1173635

4. Mattison JA, Roth GS, Beasley TM, Tilmont EM, Handy AM, Herbert RL, Longo DL, Allison DB, Young JE, Bryant M, et al. Impact of caloric restriction on health and survival in rhesus monkeys from the NIA study. Nature 2012; 489:318-21; PMID:22932268; http://dx.doi.org/10.1038/nature11432

5. Fontana L, Partridge L, Longo VD. Extending healthy life span–from yeast to humans. Science 2010; 328:321-6; PMID:20395504; http://dx.doi.org/10.1126/science.1172539

6. Hansen M, Chandra A, Mitic LL, Onken B, Driscoll M, Kenyon C. A role for autophagy in the extension of lifespan by dietary restriction in C. elegans. PLoS Genet 2008; 4:e24.

7. Eisenberg T, Knauer H, Schauer A, Buttner S, Ruckenstuhl C, Carmona-Gutierrez D, Ring J, Schroeder S, Magnes C, Antonacci L, et al. Induction of autophagy by spermidine promotes longevity. Nat Cell Biol 2009; 11:1305-14.

8. Madeo F, Eisenberg T, Buttner S, Ruckenstuhl C, Kroemer G. Spermidine: a novel autophagy inducer and longevity elixir. Autophagy 2010; 6:160-2; PMID:20110777; http://dx.doi.org/10.4161/auto.6.1.10600

9. Miller RA, Harrison DE, Astle CM, Baur JA, Boyd AR, de CR, Fernandez E, Flurkey K, Javors MA, Nelson JF, et al. Rapamycin, but not resveratrol or simvastatin, extends life span of genetically heterogeneous mice. J Gerontol A Biol Sci Med Sci 2011; 66:191-201; PMID:20974732; http://dx.doi.org/10.1093/gerona/glq178

10. Morselli E, Maiuri MC, Markaki M, Megalou E, Pasparaki A, Palikaras K, Criollo A, Galluzzi L, Malik SA, Vitale I, et al. Caloric restriction and resveratrol promote longevity through the Sirtuin-1-dependent induction of autophagy. Cell Death Dis 2010; 1:e10; PMID:21364612; http://dx.doi.org/10.1038/cddis.2009.8

11. Hariharan N, Maejima Y, Nakae J, Paik J, Depinho RA, Sadoshima J. Deacetylation of FoxO by Sirt1 Plays an Essential Role in Mediating Starvation-Induced Autophagy in Cardiac Myocytes. Circ Res 2010; 107:1470-82.

12. Mizushima N, Yamamoto A, Matsui M, Yoshimori T, Ohsumi Y. In vivo analysis of autophagy in response to nutrient starvation using transgenic mice expressing a fluorescent autophagosome marker. Mol Biol Cell 2004; 15:1101-11.

13. Zhu H, Tannous P, Johnstone JL, Kong Y, Shelton JM, Richardson JA, Le V, Levine B, Rothermel BA, Hill JA. Cardiac autophagy is a maladaptive response to hemodynamic stress. J Clin Invest 2007; 117:1782-93.

14. Komatsu M, Waguri S, Ueno T, Iwata J, Murata S, Tanida I, Ezaki J, Mizushima N, Ohsumi Y, Uchiyama Y, et al. Impairment of starvation-induced and constitutive autophagy in Atg7-deficient mice. J Cell Biol 2005; 169:425-34; http://dx.doi.org/10.1083/jcb.200412022

15. Kuma A, Hatano M, Matsui M, Yamamoto A, Nakaya H, Yoshimori T, Ohsumi Y, Tokuhisa T, Mizushima N. The role of autophagy during the early neonatal starvation period. Nature 2004; 432:1032-6; PMID:15525940; http://dx.doi.org/10.1038/nature03029

16. Kanamori H, Takemura G, Maruyama R, Goto K, Tsujimoto A, Ogino A, Li L, Kawamura I, Takeyama T, Kawaguchi T, et al. Functional significance and morphological characterization of starvation-induced autophagy in the adult heart. Am J Pathol 2009; 174:1705-14; PMID:19342365; http://dx.doi.org/10.2353/ajpath.2009.080875

17. Matsui Y, Takagi H, Qu X, Abdellatif M, Sakoda H, Asano T, Levine B, Sadoshima J. Distinct roles of autophagy in the heart during ischemia and reperfusion: roles of AMP-activated protein kinase and Beclin 1 in mediating autophagy. Circ Res 2007; 100:914-22.

18. Buss SJ, Muenz S, Riffel JH, Malekar P, Hagenmueller M, Weiss CS, Bea F, Bekeredjian R, Schinke-Braun M, Izumo S, et al. Beneficial effects of Mammalian target of rapamycin inhibition on left ventricular remodeling after myocardial infarction. J Am Coll Cardiol 2009; 54:2435-46; PMID:20082935; http://dx.doi.org/10.1016/j.jacc.2009.08.031

19. Huang C, Yitzhaki S, Perry CN, Liu W, Giricz Z, Mentzer RM, Jr., Gottlieb RA. Autophagy induced by ischemic preconditioning is essential for cardioprotection. J Cardiovasc Transl Res 2010; 3:365-73; PMID:20559777; http://dx.doi.org/10.1007/s12265-010-9189-3

20. Yan L, Vatner DE, Kim SJ, Ge H, Masurekar M, Massover WH, Yang G, Matsui Y, Sadoshima J, Vatner SF. Autophagy in chronically ischemic myocardium. Proc Natl Acad Sci USA 2005; 102:13807-12; PMID:16174725; http://dx.doi.org/10.1073/pnas.0506843102

21. Harvie MN, Pegington M, Mattson MP, Frystyk J, Dillon B, Evans G, Cuzick J, Jebb SA, Martin B, Cutler RG, et al. The effects of intermittent or continuous energy restriction on weight loss and metabolic disease risk markers: a randomized trial in young overweight women. Int J Obes(Lond) 2011; 35:714-27; PMID:20921964; http://dx.doi.org/10.1038/ijo.2010.171

22. Goodrick CL, Ingram DK, Reynolds MA, Freeman JR, Cider N. Effects of intermittent feeding upon body weight and lifespan in inbred mice: interaction of genotype and age. Mech Ageing Dev 1990; 55:69-87.

23. Ahmet I, Wan R, Mattson MP, Lakatta EG, Talan M. Cardioprotection by intermittent fasting in rats. Circulation 2005; 112:3115-21; PMID:16275865; http://dx.doi.org/10.1161/CIRCULATIONAHA.105.563817

24. Katare RG, Kakinuma Y, Arikawa M, Yamasaki F, Sato T. Chronic intermittent fasting improves the survival following large myocardial ischemia by activation of BDNF/VEGF/PI3K signaling pathway. J Mol Cell Cardiol 2009; 46:405-12.

25. Anson RM, Guo Z, de CR, Iyun T, Rios M, Hagepanos A, Ingram DK, Lane MA, Mattson MP. Intermittent fasting dissociates beneficial effects of dietary restriction on glucose metabolism and neuronal resistance to injury from calorie intake. Proc Natl Acad Sci USA 2003; 100:6216-20; http://dx.doi.org/10.1073/pnas.1035720100

26. Iwai-Kanai E, Yuan H, Huang C, Sayen MR, Perry-Garza CN, Kim L, Gottlieb RA. A method to measure cardiac autophagic flux in vivo. Autophagy 2008; 4:322-9; PMID:18216495; http://dx.doi.org/10.4161/auto.5603

27. Nishino I, Fu J, Tanji K, Yamada T, Shimojo S, Koori T, Mora M, Riggs JE, Oh SJ, Koga Y, et al. Primary LAMP-2 deficiency causes X-linked vacuolar cardiomyopathy and myopathy (Danon disease). Nature 2000; 406:906-10; PMID:10972294; http://dx.doi.org/10.1038/35022604

28. Tanaka Y, Guhde G, Suter A, Eskelinen EL, Hartmann D, Lullmann-Rauch R, Janssen PM, Blanz J, von Figura K, Saftig P. Accumulation of autophagic vacuoles and cardiomyopathy in LAMP-2-deficient mice. Nature 2000; 406:902-6; PMID:10972293; http://dx.doi.org/10.1038/35022595

29. Lyon MF. Gene action in the X-chromosome of the mouse (Mus musculus L.). Nature 1961; 190:372-3; PMID:13764598; http://dx.doi.org/10.1038/190372a0

30. Stypmann J, Janssen PM, Prestle J, Engelen MA, Kogler H, Lullmann-Rauch R, Eckardt L, von FK, Landgrebe J, Mleczko A, et al. LAMP-2 deficient mice show depressed cardiac contractile function without significant changes in calcium handling. Basic Res Cardiol 2006; 101:281-91; http://dx.doi.org/10.1007/s00395-006-0591-6

31. Bjorkoy G, Lamark T, Pankiv S, Overvatn A, Brech A, Johansen T. Monitoring autophagic degradation of p62/SQSTM1. Methods Enzymol 2009; 452:181-97; PMID:19200883

32. Korolchuk VI, Mansilla A, Menzies FM, Rubinsztein DC. Autophagy inhibition compromises degradation of ubiquitin-proteasome pathway substrates. Mol Cell 2009; 33:517-27.

33. Jaber N, Dou Z, Chen JS, Catanzaro J, Jiang YP, Ballou LM, Selinger E, Ouyang X, Lin RZ, Zhang J, et al.

Class III PI3K Vps34 plays an essential role in autophagy and in heart and liver function. Proc Natl Acad Sci USA 2012; 109:2003-8; http://dx.doi.org/10.1073/pnas.1112848109

34. Nakai A, Yamaguchi O, Takeda T, Higuchi Y, Hikoso S, Taniike M, Omiya S, Mizote I, Matsumura Y, Asahi M, et al. The role of autophagy in cardiomyocytes in the basal state and in response to hemodynamic stress. Nat Med 2007; 13:619-24.

35. Lieberman AP, Puertollano R, Raben N, Slaugenhaupt S, Walkley SU, Ballabio A. Autophagy in lysosomal storage disorders. Autophagy 2012; 8:719-30; http://dx.doi.org/10.4161/auto.19469

36. Ma X, Liu H, Foyil SR, Godar RJ, Weinheimer CJ, Hill JA, Diwan A. Impaired autophagosome clearance contributes to cardiomyocyte death in ischemia/reperfusion injury. Circulation 2012; 125:3170-81; PMID:22592897; http://dx.doi.org/10.1161/CIRCULATIONAHA.111.041814

37. Ashrafi G, Schwarz TL. The pathways of mitophagy for quality control and clearance of mitochondria. Cell Death Differ 2013; 20:31-42; PMID:22743996; http://dx.doi.org/10.1038/cdd.2012.81

38. Chen YR, Zweier JL. Cardiac mitochondria and reactive oxygen species generation. Circ Res 2014; 114:524-37; PMID:24481843; http://dx.doi.org/10.1161/CIRCRESAHA.114.300559

39. Huang C, Andres AM, Ratliff EP, Hernandez G, Lee P, Gottlieb RA. Preconditioning involves selective mitophagy mediated by Parkin and p62/SQSTM1. PLoS One 2011; 6:e20975; http://dx.doi.org/10.1371/journal.pone.0020975

40. Schneider JL, Suh Y, Cuervo AM. Deficient chaperone-mediated autophagy in liver leads to metabolic dysregulation. Cell Metab 2014; 20:417-32; PMID:25043815; http://dx.doi.org/10.1016/j.cmet.2014.06.009

41. Kiffin R, Christian C, Knecht E, Cuervo AM. Activation of chaperone-mediated autophagy during oxidative stress. Mol Biol Cell 2004; 15:4829-40.

42. Egan DF, Shackelford DB, Mihaylova MM, Gelino S, Kohnz RA, Mair W, Vasquez DS, Joshi A, Gwinn DM, Taylor R, et al. Phosphorylation of ULK1 (hATG1) by AMP-activated protein kinase connects energy sensing to mitophagy. Science 2011; 331:456-61; PMID:21205641; http://dx.doi.org/10.1126/science.1196371

43. Carreira RS, Lee Y, Ghochani M, Gustafsson AB, Gottlieb RA. Cyclophilin D is required for mitochondrial removal by autophagy in cardiac cells. Autophagy 2010; 6:462-72; PMID:20364102; http://dx.doi.org/10.4161/auto.6.4.11553

44. Yu L, McPhee CK, Zheng L, Mardones GA, Rong Y, Peng J, Mi N, Zhao Y, Liu Z, Wan F, et al. Termination of autophagy and reformation of lysosomes regulated by mTOR. Nature 2010; 465:942-6; PMID:20526321; http://dx.doi.org/10.1038/nature09076

45. Martina JA, Chen Y, Gucek M, Puertollano R. MTORC1 functions as a transcriptional regulator of autophagy by preventing nuclear transport of TFEB. Autophagy 2012; 8:903-14; PMID:22576015; http://dx.doi.org/10.4161/auto.19653

46. Roczniak-Ferguson A, Petit CS, Froehlich F, Qian S, Ky J, Angarola B, Walther TC, Ferguson SM. The Transcription Factor TFEB Links mTORC1 Signaling to Transcriptional Control of Lysosome Homeostasis. Sci Signal 2012; 5:ra42.

47. Settembre C, Di MC, Polito VA, Garcia AM, Vetrini F, Erdin S, Erdin SU, Huynh T, Medina D, Colella P, et al. TFEB links autophagy to lysosomal biogenesis. Science 2011; 332:1429-33; PMID:21617040; http://dx.doi.org/10.1126/science.1204592

48. Settembre C, Zoncu R, Medina DL, Vetrini F, Erdin S, Erdin S, Huynh T, Ferron M, Karsenty G, Vellard MC, et al. A lysosome-to-nucleus signalling mechanism senses and regulates the lysosome via mTOR and TFEB. EMBO J 2012; 31(5):1095-108; PMID:22343943

49. Palmieri M, Impey S, Kang H, di RA, Pelz C, Sardiello M, Ballabio A. Characterization of the CLEAR network reveals an integrated control of cellular clearance pathways. Hum Mol Genet 2011; 20:3852-66.

50. Sardiello M, Palmieri M, di RA, Medina DL, Valenza M, Gennarino VA, Di MC, Donaudy F, Embrione V, Polishchuk RS, et al. A gene network regulating lysosomal biogenesis and function. Science 2009; 325:473-7; PMID:19556463

51. Kuiper RP, Schepens M, Thijssen J, Schoenmakers EF, van Kessel AG. Regulation of the MiTF/TFE bHLH-LZ transcription factors through restricted spatial expression and alternative splicing of functional domains. Nucleic Acids Res 2004; 32:2315-22; PMID:15118077; http://dx.doi.org/10.1093/nar/gkh571

52. Pena-Llopis S, Vega-Rubin-de-Celis S, Schwartz JC, Wolff NC, Tran TA, Zou L, Xie XJ, Corey DR, Brugarolas J. Regulation of TFEB and V-ATPases by mTORC1. EMBO J 2011; 30:3242-58; PMID:21804531; http://dx.doi.org/10.1038/emboj.2011.257

53. Settembre C, De CR, Mansueto G, Saha PK, Vetrini F, Visvikis O, Huynh T, Carissimo A, Palmer D, Jurgen KT, et al. TFEB controls cellular lipid metabolism through a starvation-induced autoregulatory loop. Nat-Cell Biol 2013.

54. Honjoh S, Yamamoto T, Uno M, Nishida E. Signalling through RHEB-1 mediates intermittent fasting-induced longevity in C. elegans. Nature 2009; 457:726-30; PMID:19079239; http://dx.doi.org/10.1038/nature07583

55. Arum O, Bonkowski MS, Rocha JS, Bartke A. The growth hormone receptor gene-disrupted mouse fails to respond to an intermittent fasting diet. Aging Cell 2009; 8:756-60; PMID:19747233; http://dx.doi.org/10.1111/j.1474-9726.2009.00520.x

56. Ahmet I, Tae HJ, de CR, Lakatta EG, Talan MI. Effects of calorie restriction on cardioprotection and cardiovascular health. J Mol Cell Cardiol 2011; 51:263-71.

57. Sumithran P, Prendergast LA, Delbridge E, Purcell K, Shulkes A, Kriketos A, Proietto J. Long-term persistence of hormonal adaptations to weight loss. N Engl J Med 2011; 365:1597-604; http://dx.doi.org/10.1056/NEJMoa1105816

58. Wing RR. Long-term effects of a lifestyle intervention on weight and cardiovascular risk factors in individuals with type 2 diabetes mellitus: four-year results of the Look AHEAD trial. Arch Intern Med 2010; 170:1566-75.

59. Longo VD, Mattson MP. Fasting: molecular mechanisms and clinical applications. Cell Metab 2014; 19:181-92; PMID:24440038; http://dx.doi.org/10.1016/j.cmet.2013.12.008

60. Lemasters JJ. Variants of mitochondrial autophagy: Types 1 and 2 mitophagy and micromitophagy (Type 3). Redox Biol 2014; 2:749-54; PMID:25009776; http://dx.doi.org/10.1016/j.redox.2014.06.004

61. Eskelinen EL, Schmidt CK, Neu S, Willenborg M, Fuertes G, Salvador N, Tanaka Y, Lullmann-Rauch R, Hartmann D, Heeren J, et al. Disturbed cholesterol traffic but normal proteolytic function in LAMP-1/LAMP-2 double-deficient fibroblasts. Mol Biol Cell 2004; 15:3132-45.

62. Mijaljica D, Prescott M, Devenish RJ. Microautophagy in mammalian cells: revisiting a 40-year-old conundrum. Autophagy 2011; 7:673-82; PMID:21646866; http://dx.doi.org/10.4161/auto.7.7.14733

63. Nishida K, Kyoi S, Yamaguchi O, Sadoshima J, Otsu K. The role of autophagy in the heart. Cell Death Differ 2009; 16:31-8; PMID:19008922; http://dx.doi.org/10.1038/cdd.2008.163

64. Gottlieb RA, Finley KD, Mentzer RM, Jr. Cardioprotection requires taking out the trash. Basic Res Cardiol 2009; 104:169-80; http://dx.doi.org/10.1007/s00395-009-0011-9

65. Kim AS, Miller EJ, Wright TM, Li J, Qi D, Atsina K, Zaha V, Sakamoto K, Young LH. A small molecule AMPK activator protects the heart against

ischemia-reperfusion injury. J Mol Cell Cardiol 2011; 51:24-32; http://dx.doi.org/10.1016/j.amjcard.2011.02.053

66. Khan S, Salloum F, Das A, Xi L, Vetrovec GW, Kukreja RC. Rapamycin confers preconditioning-like protection against ischemia-reperfusion injury in isolated mouse heart and cardiomyocytes. J Mol Cell Cardiol 2006; 41:256-64.

67. Steingrimsson E, Tessarollo L, Reid SW, Jenkins NA, Copeland NG. The bHLH-Zip transcription factor Tfeb is essential for placental vascularization. Development 1998; 125:4607-16; PMID:9806910

68. Ma X, Liu H, Murphy JT, Foyil SR, Godar RJ, Abuirqeba H, Weinheimer CJ, Barger PM, Diwan A. Regulation of TFEB-PGC1alpha axis by beclin-1 controls mitochondrial quality and cardiomyocyte death under stress. Mol Cell Biol 2015; 35(6):956-76.

69. Syed F, Diwan A, Hahn HS. Murine echocardiography: a practical approach for phenotyping genetically manipulated and surgically modeled mice. J Am Soc Echocardiogr 2005; 18:982-90.

70. Diwan A, Krenz M, Syed FM, Wansapura J, Ren X, Koesters AG, Li H, Kirshenbaum LA, Hahn HS, Robbins J, et al. Inhibition of ischemic cardiomyocyte apoptosis through targeted ablation of Bnip3 restrains postinfarction remodeling in mice. J Clin Invest 2007; 117:2825-33.

71. Chen Y, Lewis W, Diwan A, Cheng EH, Matkovich SJ, Dorn GW. Dual autonomous mitochondrial cell death pathways are activated by Nix/BNip3L and induce cardiomyopathy. Proc Natl Acad Sci USA 2010; 107:9035-42; http://dx.doi.org/10.1073/pnas.0914013107

72. Zhao J, Brault JJ, Schild A, Cao P, Sandri M, Schiaffino S, Lecker SH, Goldberg AL. FoxO3 coordinately activates protein degradation by the autophagic/lysosomal and proteasomal pathways in atrophying muscle cells. Cell Metab 2007; 6:472-83; PMID:18054316; http://dx.doi.org/10.1016/j.cmet.2007.11.004

73. Komatsu M, Waguri S, Koike M, Sou YS, Ueno T, Hara T, Mizushima N, Iwata J, Ezaki J, Murata S, et al. Homeostatic levels of p62 control cytoplasmic inclusion body formation in autophagy-deficient mice. Cell 2007; 131:1149-63; PMID:18083104; http://dx.doi.org/10.1016/j.cell.2007.10.035

74. Zhang H, Bosch-Marce M, Shimoda LA, Tan YS, Baek JH, Wesley JB, Gonzalez FJ, Semenza GL. Mitochondrial autophagy is an HIF-1-dependent adaptive metabolic response to hypoxia. J Biol Chem 2008; 283:10892-903.

75. Yanagawa M, Tsukuba T, Nishioku T, Okamoto Y, Okamoto K, Takii R, Terada Y, Nakayama KI, Kadowaki T, Yamamoto K. Cathepsin E deficiency induces a novel form of lysosomal storage disorder showing the accumulation of lysosomal membrane

sialoglycoproteins and the elevation of lysosomal pH in macrophages. J Biol Chem 2007; 282:1851-62.

76. Sferruzzi-Perri AN, Macpherson AM, Roberts CT, Robertson SA. Csf2 null mutation alters placental gene expression and trophoblast glycogen cell and giant cell abundance in mice. Biol Reprod 2009; 81:207-21.

77. Ma X, Godar RJ, Liu H, Diwan A. Enhancing lysosome biogenesis attenuates BNIP3-induced cardiomyocyte death. Autophagy 2012; 8:297-309; PMID:22302006; http://dx.doi.org/10.4161/auto.18658

78. Yang KC, Ma X, Liu H, Murphy J, Barger PM, Mann DL, Diwan A. TNF-receptor associated factor-2 mediates mitochondrial autophagy. Circ Heart Fail 2014; 8 (1):175-87.

79. Huang dW, Sherman BT, Lempicki RA. Systematic and integrative analysis of large gene lists using DAVID bioinformatics resources. Nat Protoc 2009; 4:44-57.

80. Huang dW, Sherman BT, Lempicki RA. Bioinformatics enrichment tools: paths toward the comprehensive functional analysis of large gene lists. Nucleic Acids Res 2009; 37:1-13; PMID:19033363; http://dx.doi.org/10.1093/nar/gkn923

81. Goonasekera SA, Hammer K, Auger-Messier M, Bodi I, Chen X, Zhang H, Reiken S, Elrod JW, Correll RN, York AJ, et al. Decreased cardiac L-type Ca(2)(+) channel activity induces hypertrophy and heart failure in mice. J Clin Invest 2012; 122:280-90.